CHAPTER FIVE

Three types of pyroclastic deposits and their eruption: an introduction

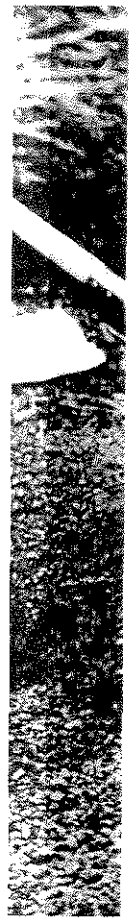

) 1065, San
egates – so

Initial statement

Pyroclastic deposits form directly from the fragmentation of magma and rock by explosive volcanic activity. They can be grouped into three genetic types according to their mode of transport and deposition:

falls
flows
surges

In this introductory chapter on pyroclastic rocks we set out the differences between these three basic types of deposit. We also describe the eruption style and the deposits of different kinds of pyroclastic falls, flows and surges, based on studies of Quaternary volcanoes. Recent work on pyroclastic deposits from modern volcanic successions has largely concentrated on their genesis, and here we relate the deposits to the physical processes controlling their formation, transportation and deposition. Accretionary lapilli receive special mention, since these can be important indicators of certain types of eruption and process, and for distinguishing pyroclastic deposits from other volcaniclastic sediments.

5.1 Introduction

Three basic types of pyroclastic deposit have been distinguished in the literature:

pyroclastic fall deposits
pyroclastic flow deposits
pyroclastic surge deposits

These types can all be formed by any of the

pyroclastic explosive eruption mechanisms introduced in Chapter 3 (magmatic, phreatomagmatic and phreatic). The essential characteristics of the main pyroclastic deposit types are initially summarised here, before their more detailed description and discussion in the later sections below, and in subsequent chapters (Chs 6–9). The components found in pyroclastic deposits have been described in Chapter 3. The approach and methods used to study and analyse modern pyroclastic deposits are described and discussed in Appendix I. Particularly relevant to this chapter is the discussion on grainsize distribution in Appendix I.

5.1.1 PYROCLASTIC FALL DEPOSITS: DEFINITION

A fall deposit is formed after material has been explosively ejected from a vent, producing an eruption column, which is a buoyant plume of tephra and gas rising high into the atmosphere. The geometry and size of a deposit reflects the eruption column height, and the velocity and direction of

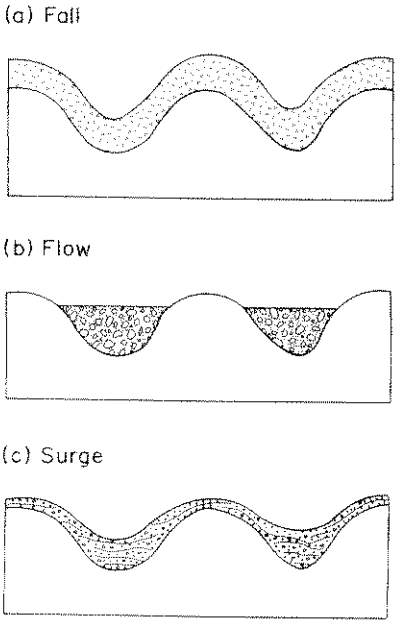

Figure 5.1 Geometric relationships of the three basic types of pyroclastic deposit overlying the same topography. (After J. V. Wright *et al.* 1980.)

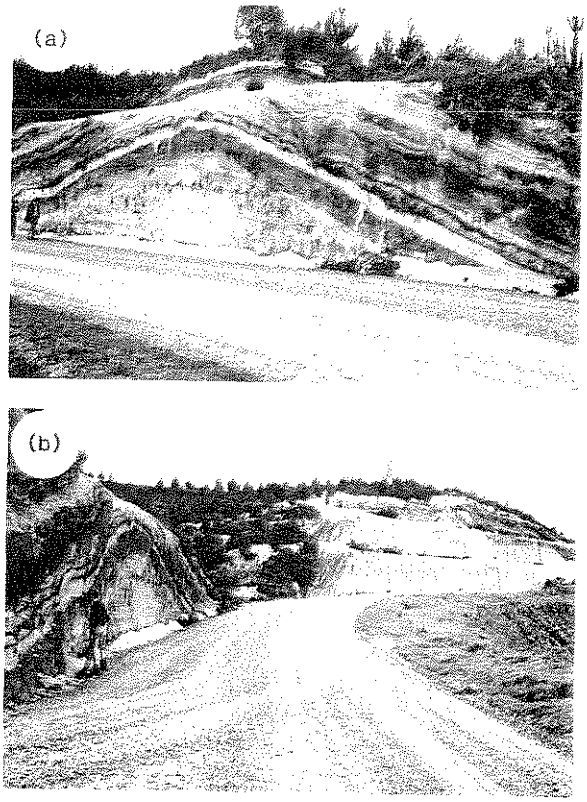

Figure 5.2 Several separate pyroclastic fall deposits forming the bedded sequence mantling erosional topography. Hills and valleys are cut into older massive pumiceous pyroclastic flow deposits of the Oruanui ignimbrite (20 000 years BP), near Lake Taupo, New Zealand.

atmospheric winds (G. P. L. Walker 1973b, L. Wilson *et al.* 1978). As the plume expands, pyroclasts fall back to Earth, under the influence of gravity, at varying distances downwind from the source, depending on their size and density (or terminal fall velocity; Ch. 6) so forming *eruption plume derived fall deposits*. The largest fragments will be explosively ejected on ballistic trajectories, and these are unaffected by the wind and are called *ballistic clasts*. Other fine-grained pyroclastic fall deposits are generated in part from ash elutriated out of the top of moving pyroclastic flows forming *ash-cloud derived fall deposits*; examples of this type of pyroclastic fall deposit can be more voluminous and may be further dispersed than those of ash from eruption columns (Section 5.2).

leposits form-
topography.
e pumiceous
ignimbrite
land.

1973b, L.
e expands,
influence of
id from the
density (or
ing *eruption*
t fragments
trajectories,
id are called
oclastic fall
h elutriated
ws forming
of this type
voluminous
ose of ash

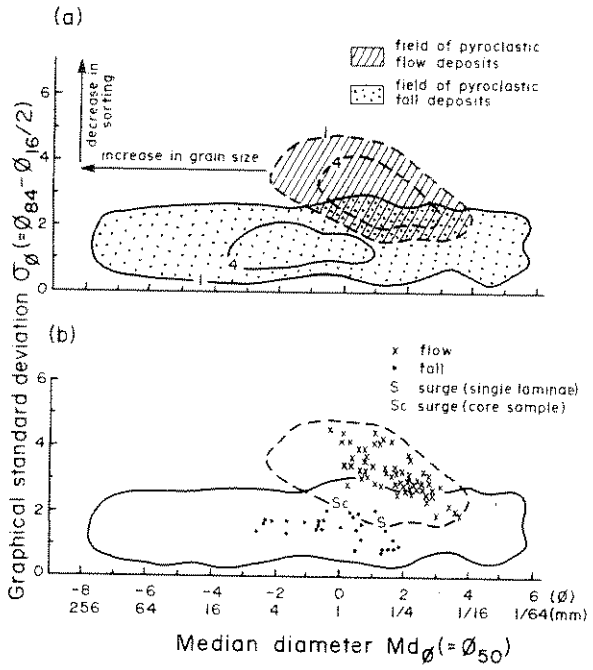

Figure 5.3 (a) Md_ϕ/σ_ϕ plot often used to show grainsize characteristics of unconsolidated modern pyroclastic deposits. The grainsize distribution of a sample is first determined by mechanical analysis (App. I). Cumulative curves of the distribution are then drawn on arithmetic probability paper and the two Inman (1952) parameters of median diameter and graphical standard deviation, which is a measure of sorting, are derived. Solid lines labelled 1% and 4% are contours for the field of pyroclastic fall deposits and within these 99% and 96%, respectively, of sieve analyses of fall deposits occur (based on over 1300 analyses) (after G. P. L. Walker 1971). Broken lines are similar contours for the field of pyroclastic flow analyses (based on about 800 analyses) (after G. P. L. Walker 1971, G. P. L. Walker *et al.* 1980). (b) Example of an Md_ϕ/σ_ϕ plot. All of the samples are from the products of one large Mexican eruption. This produced pumiceous pyroclastic fall, surge and flow deposits. The pyroclastic flow deposits are called the Rio Caliente ignimbrite (after J. V. Wright 1981).

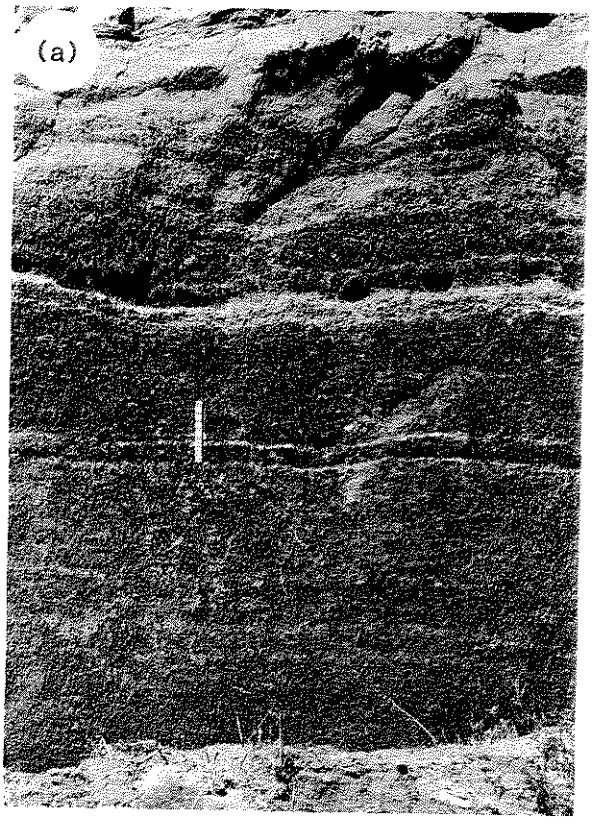

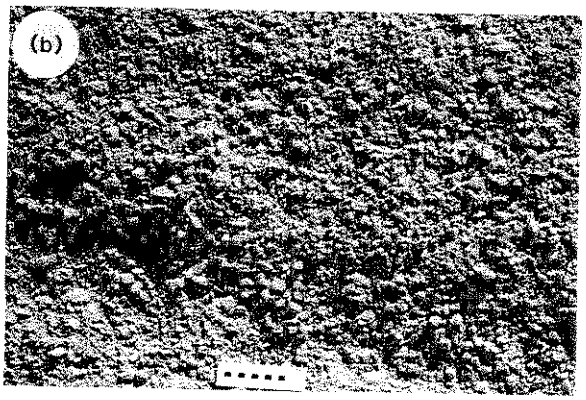

Figure 5.4 Two pyroclastic fall deposits. (a) Scoria fall deposit on Santorini. Note planar stratification and the degraded top of the deposit which is a palaeosol. Rule is 30 cm long. (b) Close-up, showing good sorting (for a pyroclastic deposit) of a pumice-fall deposit from the Lower Bandelier Tuff, New Mexico (Ch. 6).

Fall deposits show **mantle bedding**; that is, they locally maintain a uniform thickness while draping all but the steepest topography (Figs 5.1 & 2). Although pyroclastic deposits are generally poorly sorted, fall deposits are relatively well sorted (σ_ϕ values are normally $\leqslant 2.0$, Figs 5.3 & 4) because of aeolian fractionation during transport. Sometimes they show planar internal stratification or lamination (which has been called shower bedding; Fig. 5.4a) due to variations in eruption column behaviour, but never cross-stratification or bedforms showing erosion or truncation of the underlying layers. Near to the vent, some air-fall deposits are welded, or pass into agglutinated spatter (Ch. 3). Carbonised wood is generally lacking but, when found, is usually restricted to near-vent deposits.

5.1.2 PYROCLASTIC FLOW DEPOSITS: DEFINITION

These are the deposits left by surface flows of pyroclastic debris which travel as a high particle concentration gas–solid dispersion. They are gravity controlled, hot and, in some instances, may be partly fluidised (Ch. 7). As a general rule, deposits are topographically controlled, filling valleys and depressions (Figs 5.1, 5 & 6). However, certain '*violent*' pumiceous pyroclastic flows emplaced at extremely high velocities are known to form a topography mantling pyroclastic flow facies. We will discuss this special facies in Chapter 7.

Internally, pyroclastic flow deposits are generally massive and poorly sorted ($\sigma_\phi \geqslant 2.0$), but sometimes show grading of larger clasts known as coarse-tail grading (Fig. 5.6). Poor sorting in flow deposits is attributed to high particle concentration, and not to turbulence, with the dominant flow mechanisms probably being laminar or plug flow, or both (Ch. 7). The superposition of a number of flow units (each flow unit being regarded as the deposit of a single pyroclastic flow) can give the appearance of internal stratification (e.g. Fig. 5.16a, below); however, a diffuse layering is occasionally observed within individual flow units, and is due to internal shearing during transport. Pyroclastic flow deposits sometimes contain '*fossil fumarole pipes*' or gas segregation pipes (e.g. Fig. 5.15c, below), from

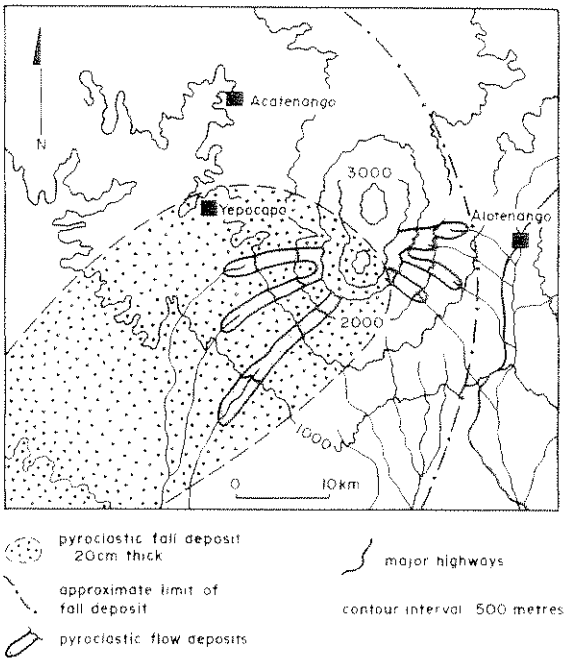

Figure 5.5 Distribution of pyroclastic flow deposits from the 1974 eruption of Fuego volcano, Guatemala. The pyroclastic flow deposits fill canyons and valleys on the lower slopes of the volcano. Their distribution contrasts with the pyroclastic fall deposits produced in the same eruption. (After D. K. Davies *et al.* 1978a, Rose *et al.* 1978.)

which the fine-ash fraction has been lost by gas streaming through the moving pyroclastic flow, or after the flow came to rest (C. J. N. Wilson 1980; Ch. 7). Such gas streaming produces pipes and other pods enriched in heavier crystals, lithics or larger vesicular fragments, which are important features that distinguish these primary pyroclastic mass-flow deposits of pyroclastic debris from epiclastic flows of volcanic material.

Pyroclastic flows are emplaced at high temperatures (Table 5.1). Evidence for a high emplacement temperature is also very important in distinguishing pyroclastic flow deposits from epiclastic debris flow deposits. This evidence would include the presence of:

(a) carbonised wood,
(b) pink coloration due to thermal oxidation of iron, or dark coloration due to crystallisation of finely-disseminated microlites of magnetite

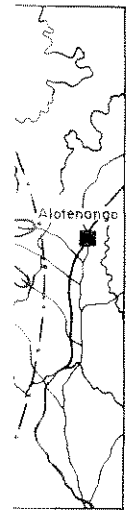

ighways

al 500 metres

eposits from
temala. The
lleys on the
ontrasts with
me eruption
78).

losi by gas
tic flow, or
ilson 1980;
pipes and
, lithics or
important
pyroclastic
from epi-

h tempera-
placement
tinguishing
debris flow
e presence

xidation of
stallisation
magnetite

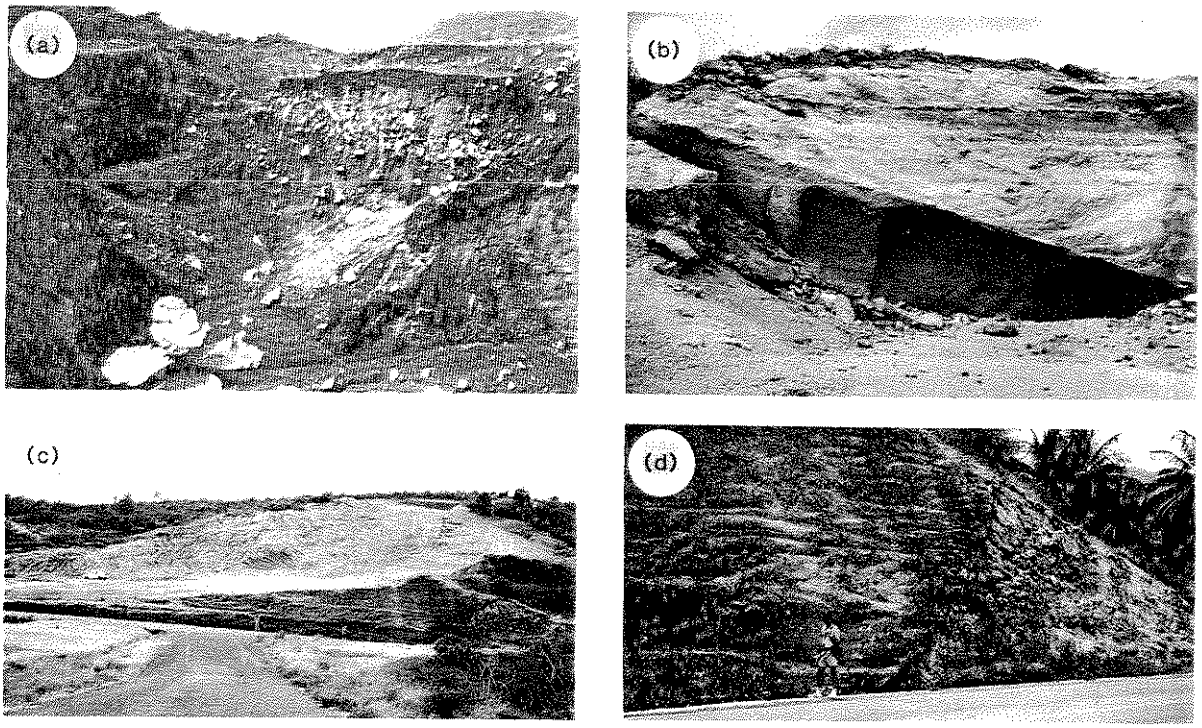

Figure 5.6 Pyroclastic flow deposits. (a) Filling a valley on the lower slopes of Fuego after the 1974 eruption (Fig. 5.5). Note the poor sorting and the large lava blocks showing overall reverse grading. The new channel cut through these deposits is approximately 40 m deep, and this was incised in two wet seasons (after Vessell & Davies 1981). (b) Pumiceous pyroclastic flow deposit (ignimbrite) ponded over a steeply dipping pumice-fall deposit. The pumice-fall deposit mantles former topography and is internally stratified. This is called the Granadilla pumice, and the pyroclastic flow was erupted later in the same eruption on Tenerife. A younger, thin pumice-fall deposit overlies the flat top of the pyroclastic flow deposit and this is capped by a palaeosol (photograph by J. A. Wolff). (c) and (d) Thick deposit of a single pumice flow which choked a large valley cut into older volcanics at Micoud, St Lucia, Lesser Antilles. Contact is to the right of scale figures.

Table 5.1 Some measured emplacement temperatures of pyroclastic flow deposits

Deposit	Temperature (°C)	Method	Source
Komagatake 1929 pyroclastic flow deposit	390 (12 days after eruption)	direct measurement	Kozu (1934)
Mt St Helens 1981 pumice-flow deposits	300–750 (near vent 750–850)	direct measurement	Banks and Hoblitt (1981)
Vesuvius AD 79 ignimbrite	~400	palaeomagnetic & infra-red spectrum of carbonised wood	D. V. Kent *et al.* (1981)
Upper Bandelier ignimbrite	550–800	welding experiments	R. L. Smith and Bailey (1966), Ch. 8
Prehistoric Mt St Helens block- and ash-flow deposit	550–600	palaeomagnetic	Hoblitt and Kellogg (1979)

(or other iron or manganese oxide minerals), which may be oxidised to haematite, producing the pink colour,
(c) a zone(s) of welded tuff and
(d) a thermal remanent magnetism (TRM; Hoblitt & Kellogg 1979).

Carbonised wood is common in pyroclastic flows erupted from volcanoes in tropical or wooded temperate areas, but is absent or scarce in those erupted from volcanoes in dry climates.

Although the term 'ignimbrite' is widely used for the deposit of any pyroclastic flow, we reserve it for the deposits of pumiceous pyroclastic flows (see Section 5.4.2 and Ch. 7).

5.1.3 PYROCLASTIC SURGE DEPOSITS: DEFINITION

A surge transports pyroclasts along the surface as an expanded, turbulent, low particle concentration gas–solid dispersion. Deposits mantle topography but are also topographically controlled, and they tend to accumulate, or are thickest in depressions (Fig. 5.1). Characteristically, they show unidirectional sedimentary bedforms: low angle cross-stratification, dune-forms, climbing dune-forms, pinch and swell structures, and chute and pool structures have all been described. Deposits are often enriched in denser lithics and crystals. Individual laminae are generally well sorted, but core samples incorporating a number of laminae can be poorly sorted (Fig. 5.3). They can contain small gas segregation pipes, produced by gases escaping from preceding flow deposits, and carbonised wood.

Of course, surges are a type of flow, but the term pyroclastic flow has traditionally been associated with the high concentration flows, and it is appropriate to classify the fundamentally different types of deposits produced by flows and surges separately, even though there may essentially be a spectrum (see Ch. 7 for further discussion on the distinction, and the debate surrounding this).

5.2 Eruptions producing pyroclastic falls

Upward transport of pyroclasts high into the Earth's atmosphere may occur in two ways:

in eruption columns accompanying explosive eruptions
in ash clouds accompanying pyroclastic flows.

5.2.1 EXPLOSIVE ERUPTION COLUMNS

The eruption columns produced by explosive eruptions may take many forms (Figs 5.7 & 8), and their energetics and dynamics have been discussed recently by Settle (1978), L. Wilson *et al.* (1978), Sparks and L. Wilson (1982) and Sparks (1986). The height reached by an eruption column, together with the atmospheric wind velocity profile (which may vary with height, e.g. Fig. 13.28), controls the dispersal of pyroclasts (Fig. 5.8). Observed eruption columns have attained heights between 2 and 45 km (Table 5.2; L. Wilson *et al.* 1978). Plume height is a function of vent radius, gas exit velocity, gas content of the eruption products and the efficiency of conversion of thermal energy during the entrainment of cool atmospheric air (L. Wilson *et al.* 1978). In all highly explosive eruptions, the thermal energy released is completely dominant over the initial kinetic energy released from decompression and expansion of the gas phase. The style of explosive activity is also important in controlling the character of the eruption column. Discrete instantaneous explosions produce transient plumes, whereas prolonged release of fragmented magma in a steady state eruption forms a long-term, maintained plume. If discrete explosions occur in rapid succession (within seconds to a few minutes) a maintained plume may also form.

Eruption columns can be divided into three parts (Sparks & L. Wilson 1976, Sparks 1986):

(a) an initial gas thrust part, due to rapid decompression of the gas phase,
(b) an upper convection plume which is driven by the release of thermal energy from juvenile particles. In this region buoyancy is dominant and the top is defined by the level of neutral

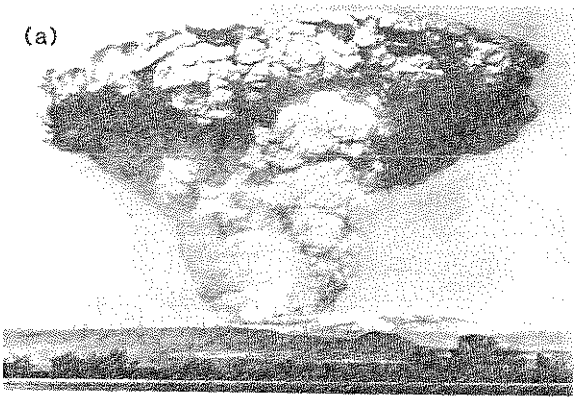

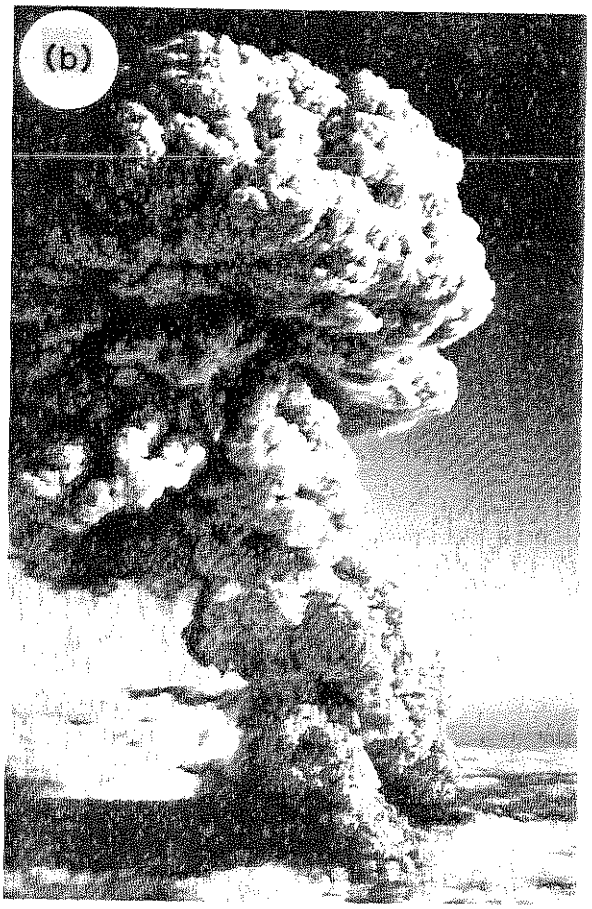

Figure 5.7 Two explosive eruption columns. (a) The 'big umbrella' or 'mushroom' above Lassen Peak, northern California, in the eruption of 22 May 1915. Eyewitness reports indicate that the height of the column was of the order of 10–15 km (photograph courtesy of Loomis Museum Association). (b) Above Mt St Helens on 22 July 1980. This shows the convective column mushrooming out, and a cloud of ash rising from a pyroclastic flow which moved towards the photographer. Column height is about 15 km (after J. W. Vallance in Christiansen & Peterson 1981).

buoyancy, H_B, where the column bulk density equals that of the surrounding atmosphere and

(c) an umbrella region (also called a downwind plume), where the column spreads radially or downwind, or both, to form an umbrella cloud. The umbrella cloud extends from height H_B to height H_T, the level to which the column continues to rise due to its momentum (Sparks 1986).

The height of the initial gas thrust phase varies with the style of the activity (Ch. 6). In most eruption columns, the lower gas thrust part makes up less than 10% of the total column height (L. Wilson *et al.* 1978). For discrete explosions (strombolian and vulcanian eruptions; Ch. 6) this ranges from a few tens of metres to a few hundred metres (E. Blackburn *et al.* 1976, Self *et al.* 1979). For maintained eruption columns the range is from a few hundred metres to a few kilometres in some eruptions (1.5–4.5 km for initial gas velocities of 400–600 m s^{-1}; L. Wilson 1976, Sparks & L. Wilson 1976). Rapid deceleration of the gas thrust phase occurs between these heights, above which particles are incorporated into an eruption column driven by convection. A maintained convecting eruption column could reach heights of greater than 40 km during some large explosive (plinian) eruptions (L. Wilson *et al.* 1978). A convecting plume will rise until it reaches a level in the atmosphere (H_B) with the same density, and then it will mushroom, spreading radially or laterally, or both, downwind (Figs 5.8 & 9). In eruption columns that form from discrete explosions, convective recovery only takes columns to heights of a few kilometres,

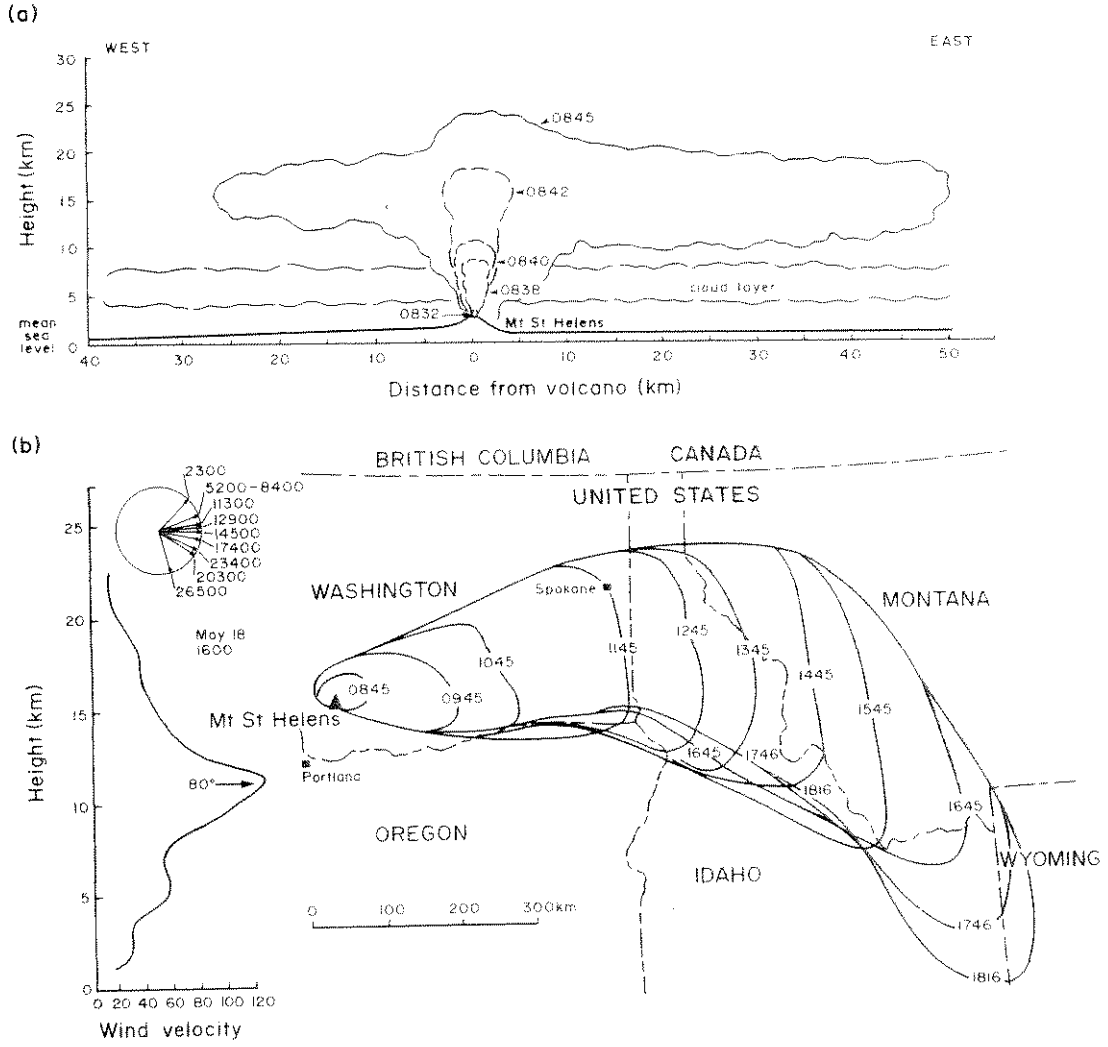

unless explosions occur in quick succession, in which case a maintained plume forms.

L. Wilson *et al.* (1978) and Settle (1978) have independently shown that the maximum height of an eruption column (H_T) is proportional to the fourth root of the rate of release of energy, and hence the fourth root of the mass eruption rate. For maintained eruption columns the height can be predicted from

$$H_T = 8.2\dot{Q}^{1/4} \qquad (5.1)$$

(after Morton *et al.* 1956, L. Wilson *et al.* 1978), where H_T is the height of the column in metres and $\dot{Q}$ is the steady rate of release of energy in watts. $\dot{Q}$ is related to the eruption conditions at vent by:

$$\dot{Q} = \beta v \pi r^2 s(\theta - \theta_a)F \qquad (5.2)$$

in which β, v, s and θ are, respectively, the bulk density, velocity, specific heat and temperature of the erupting fluid, θ_a is the temperature to which the eruption products ultimately cool (~270 K in most cases), r is the vent radius and F is an efficiency factor (discussed below). The bulk density, β, is related to the density of the magmatic gas,

(c)

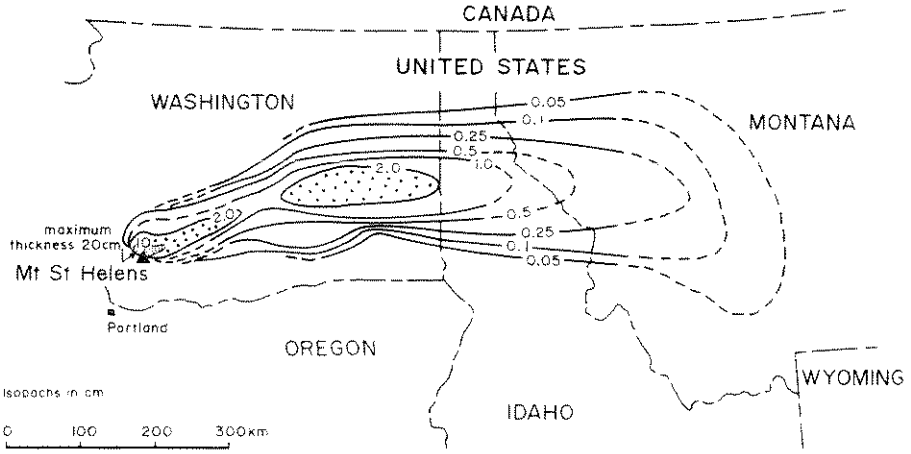

Figure 5.8 Development of the eruption column, downwind plume and dispersal of pyroclasts in the 18 May 1980 eruption of Mt St Helens. (a) East–west profile schematically showing early vertical growth and lateral expansion of the plume. (b) Isochron map showing maximum downwind extent of the edge of the plume carried by the fastest-moving wind layer (as observed on satellite photographs). On the left an average wind speed profile measured at Spokane at 16.00 h is given. Circular wind diagram shows average directions to which wind was blowing at different altitudes, and were again measured at Spokane at 16.00 h. (c) Isopachs of the 18 May pyroclastic fall deposit. Note the secondary thickening of the air-fall deposit 300 km downwind; the significance of this will be discussed in Chapter 6. (After Sarna-Wojcicki *et al.* 1981.)

Table 5.2 Some data on observed eruption columns.

Eruption	Average volumetric eruption rate ($m^3\ s^{-1}$)	Plume height (km)	Duration (h)
Hekla 1947	17 000	24	0.5
Hekla 1970	3333	14	2
Soufriere 1902	11–15 000	14.5–16	2.5–3.5
Bezymianny 1956	230 000	34–45	0.5
Fuego 1971	640	10	10
Heimaey 1973	50	2–3	
Ngauruhoe 1974	10	1.5–3.7	14
Santa Maria 1902	120 000	28	18–20
Mt St Helens			
18 May 1980	6200	16	9
Soufrière			
22 April 1979	12 600	18	0.23

Volumetric eruption rates are given in terms of dense rock equivalent (App. II).
Plume heights are above the top of the volcano, not sea level.
The data on Hekla 1947, refer to the first 30 min of the eruption.
The data on Heimaey refer to the first few weeks of the eruption.
Information is taken largely from L. Wilson *et al.* (1978), with data on Santa Maria (1902) from S. N. Williams and Self (1983), Mt St Helens (1980) from Harris *et al.* (1981) and Sarna-Wojcicki *et al.* (1981), and Soufriere, St Vincent (1979) from Sparks and L. Wilson (1982).

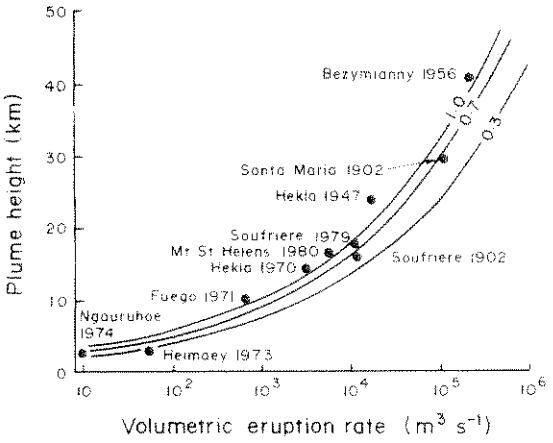

Figure 5.9 Relationship between plume height and volumetric eruption rate. The theoretical curves for F values of 1.0, 0.7 and 0.3 are discussed in the text. Observed plume heights for ten eruptions are plotted from Table 5.1. (After L. Wilson *et al.* 1978.)

ϱ_g, the density of the pyroclasts, ϱ_m, and the weight fractions of gas and pyroclasts, N and x_m:

$$\frac{1}{\beta} = \frac{x_m}{\varrho_m} + \frac{N}{\varrho_g} \qquad (5.3)$$

If it is assumed that the predominant gas is water and that the erupting fluid is at atmospheric pressure, then for $\theta = 1200$ K, ϱ_g is 0.18 kg m^{-3}. The thermal properties of magma are dominated by the solid phase for gas contents of a few per cent by weight, and the value of s, the specific heat, is taken as 1.1×10^{-3} J kg^{-1} K^{-1}.

The maximum height of the eruption column, H_T, can also be expressed as a function of the volume discharge rate of magma (Sparks 1986; Fig. 5.9):

$$H_T = 5.773(1 + n)^{-3/8}[\sigma\phi s(\theta - \theta_a)]^{\frac{1}{4}} \qquad (5.4)$$

where ϕ is the volume discharge rate in cubic metres per second, s is the specific heat, θ is the initial temperature of the erupting material, θ_a is the atmospheric temperature at sea level, σ is the magma density and n is the ratio of the vertical gradient of the absolute temperature to the lapse rate.

Figure 5.9 depicts theoretical curves showing the relationships between maintained eruption column height and volumetric eruption or discharge rate of magma calculated from Equations 5.1–5.3, together with the heights of some observed eruption columns (Table 5.1). The calculations coincide well with recorded column heights. The efficiency factor, F, measures the efficiency of conversion of heat to potential or kinetic energy, and curves with values of $F = 1.0$, 0.7 and 0.3 are used in Figure 5.9. F is mainly controlled by the degree of fragmentation of the magma in the explosive event. Here we are only considering magmatic eruptions, not the special case of explosions generated by magma–water interaction (which will be discussed below). In eruptions which generate a higher proportion of ash-sized ejecta, virtually all of the magmatic heat can be converted to mechanical energy. Many plinian deposits have a substantial proportion of fine-grained particles, and Sparks and L. Wilson (1982) estimated at least 70% efficiency in the conversion of heat in selected plinian columns. On the other hand, strombolian eruptions produce a comparatively much higher proportion of coarse debris (because of a lower degree of fragmentation: Ch. 6), and columns are likely to be much less efficient in the conversion of heat. Consequently, observed eruption columns from this type of activity should fit a theoretical curve with a low F-value, and this seems to be the case for the 1973 Heimaey eruption in Iceland (Fig. 5.9).

The maximum theoretical height expected for a stable maintained eruption plume is about 55 km (L. Wilson *et al.* 1978). This corresponds to an initial gas velocity of 700 m s^{-1} (greater muzzle velocities are unlikely to occur on Earth; McGetchin & Ullrich 1973, L. Wilson 1976), which leads to a volume eruption rate of 1.1×10^6 m^3 s^{-1}.

Equation 5.1 strictly applies to the vertical rise of an eruption column into a still atmosphere with no wind. This should be broadly applicable to most large explosive eruptions, where upward velocities of a particle-rich plume are likely to be much greater over much of its height than the transverse wind velocity. For strong winds and moderate to small eruption columns the effect of wind on column height can be significant, and this is discussed by Settle (1978). A standard atmosphere with a vertical decrease in temperature (environ-

mental lapse rate) of 6.5°C km^{-1} is also used in the calculations of the theoretical curves in Figure 5.9. However, substantial departures from standard atmosphere can occur, and the scatter in the data from observed eruptions in Figure 5.9 may partly reflect variations in vertical atmospheric temperature gradients (L. Wilson *et al.* 1978). These effects have again been illustrated by Settle (1978).

To estimate the rise height of a plume generated from a discrete explosion, another equation must be used:

$$H_T = 1.37Q^{1/4} \qquad (5.5)$$

(Morton *et al.* 1956). This has the same form as Equation 5.1, but Q is the total energy released in joules.

During phreatomagmatic eruptions, a great deal of heat, that in normal magmatic eruptions would be used to drive a convective plume, is used instead in the conversion of water to steam (the heat of vaporisation of water is 580 cal g^{-1} (1 cal ≃ 4.18 J) at atmospheric pressure and 298 K) (L. Wilson *et al.* 1978, Self & Sparks 1978). The thermal energy used in vaporisation can only be recovered by condensation of the steam. Consequently, eruption column heights should be lower in a phreatomagmatic eruption than in a magmatic eruption with the same volumetric rate of discharge. Sparks and L. Wilson (1982) indicated that the effects of steam in controlling column height are probably small except where the mass of steam is comparable with the mass of ash.

5.2.2 ASH CLOUDS ACCOMPANYING PYROCLASTIC FLOWS

During pyroclastic flow-forming eruptions, much of the explosively ejected fragmented magma particles may fail to be included in the resulting pyroclastic flow deposit. Hay (1959) first showed that an enrichment of crystals took place in a small basaltic andesite pyroclastic flow from the 1902 eruption of Soufrière, St Vincent, and he attributed this to the selective loss of vitric ash. Lipman (1967) found a similar enrichment in crystals in a pumiceous rhyolitic ignimbrite erupted from Aso caldera, Japan. Since these studies, G. P. L. Walker (1972) and Sparks and Walker (1977) have demonstrated that enrichment of crystals is a typical feature of ignimbrites, and must be accounted for by substantial volumetric losses of the vitric component of the original magma which is deposited in associated air-fall ash deposits. Much of this ash is elutriated out of the moving pumice flows by gas streaming through and up, out of the flows. The ash rises above the pumice flows in an upper turbulent ash cloud, which is taken to great heights by huge convective plumes (Fig. 5.7b). Because the ash particles are very fine-grained (nearly all <1 mm), there may be nearly 100% efficiency of conversion of heat to convective energy to drive the plumes.

The types of air-fall ash deposits which result are variously termed *layer 3 deposits* (Sparks *et al.* 1973), *co-ignimbrite ash-fall deposits* (this is our preferred term; Sparks & Walker 1977), and *vitric air-fall ash deposits* (J. V. Wright *et al.* 1980). What is significant here is that these deposits can be very extensive, and can have volumes which are comparable with those of ignimbrites. It is now thought that many of the extensive large ash layers found in deep sea cores are of this type (e.g. Ninkovich *et al.* 1978, Sparks & Huang 1980). We will describe co-ignimbrite ash-fall deposits in more detail in Chapter 8, but will first consider other types of deposits from ash clouds associated with pyroclastic flows (Section 5.6.2).

As a final comment on eruptions producing pyroclastic falls, the high plumes generated, particularly during plinian-type and ignimbrite-forming eruptions, must penetrate the level of the tropopause in the atmosphere (at heights of <6 to 18 km, depending on latitude and season) and contribute fine ash and gaseous species to stratospheric dust veils. Some climatologists have therefore thought that volcanic eruptions might promote periods of climatic cooling. The topic is beyond the scope of this book, but two critical reviews, by Rampino *et al.* (1979) and Self *et al.* (1981), have suggested that volcanic dust veils are only likely to cause short-term (<10 years) very minor temperature fluctuations (in the order of <0.5°C), and are unlikely to trigger ice ages or glaciations, or even minor fluctuations in the 10–100 year range.

Rampino *et al.* (1979) even suggested that it may be climatic variations (leading to stress changes in the Earth's crust) that augment volcanic eruptions rather than vice versa.

5.3 Pyroclastic fall deposits: types and description

The description and interpretation of pyroclastic fall deposits can be approached in a number of ways. The most useful for the volcanologist working on modern pyroclastic deposits has been the quantitative scheme of G. P. L. Walker (1973b), and we will use this as a basis for a detailed description of pyroclastic fall deposits and their explosive mechanisms in Chapter 6. This is a genetic scheme and divides explosive magmatic eruptions from open vents into two groups. The first represents a spectrum of increasing dispersal and fragmentation: **hawaiian**, **strombolian**, **subplinian**, **plinian** and **ultraplinian**. **Phreatomagmatic** eruptions constitute the second group, for which two types have been described: **surtseyan** and **phreatoplinian**. These two types have extremely high degrees of fragmentation, and are, respectively, generally basic to intermediate, and acidic in composition although air-fall type and composition cannot be considered in mutually exclusive terms. **Vulcanian** air-fall deposits generated by explosion from closed vents are also defined in the scheme.

However, before discussing this scheme and the resultant deposits (Ch. 6), are there any simpler divisions we can use that still retain some genetic considerations to distinguish modern pyroclastic fall deposits in the field? Three types of pyroclastic fall deposits can be distinguished on broad lithological and genetic grounds:

(a) scoria-fall deposits,
(b) pumice-fall deposits,
(c) ash-fall deposits.

Scoria-fall deposits are composed largely of vesiculated basalt to basaltic andesite magma (Fig. 5.4a). These are the deposits characteristic of hawaiian and strombolian explosive activity (Ch. 6). Near the vent they are associated with lava spatter cones and scoria cones. They can be very coarse-grained, with the predominant grain size >64 mm, and contain large ballistic bombs, including irregularly shaped bombs and spatter fragments (Ch. 3). Away from the cones, scoria fall deposits are finer-grained and usually <5 m thick.

Pumice-fall deposits (Fig. 5.4b) are composed largely of vesiculated high viscosity magmas (andesite to rhyolite, phonolite and trachyte). They form widely dispersed sheets, and are the sub-plinian, plinian and ultraplinian deposits in Walker's scheme (Ch. 6). Deposits of one eruption are rarely >10 m thick, but very close to the vent deposits as thick as 25 m are known. At vent, the predominant grainsize may be >64 mm, and the deposits contain large lithic and pumice blocks and bombs.

Ash-fall deposits can be formed by a whole spectrum of pyroclastic processes. Phreatomagmatic eruptions characteristically form fine-grained deposits and these often contain accretionary lapilli (Section 5.8). Co-ignimbrite ash-fall deposits can be very extensive examples. They may also contain accretionary lapilli caused by rain flushing, and would be difficult to distinguish from silicic phreatomagmatic (phreatoplinian) ash-fall deposits in the absence of field criteria (Ch. 6). Dense-clast pyroclastic flows may produce equivalent lithic ash-fall deposits. Vulcanian eruptions typically produce ash-fall deposits which may range from dense lithic-rich to scoriaceous types. Close to the vent, these deposits may contain abundant ballistic blocks and bombs. Phreatic eruptions produce lithic ash-fall deposits, and ballistic blocks may be very abundant around the vent. As well as these, pumice and scoria fall deposits have ash-fall deposits as their distal equivalents, and their character depends on downwind aeolian fractionation processes. Air-fall ash deposits range in thickness from <1 mm near vent, to >1 m thick more than 100 km away for co-ignimbrite ash-fall deposits and phreatoplinian deposits.

An alternative non-genetic approach uses lithological descriptions based on dominant grainsize and component types, as shown in Tables 12.5 & 7. For example, in this case most pumice-fall deposits would be pumice lapilli deposits. Most of the coarser near-vent equivalents of the deposits dis-

cussed above would then be called volcanic breccias. We will discuss the use of these two terms in Chapter 12.

5.4 Pyroclastic flow-forming eruptions

Pyroclastic flows (Fig. 5.10) are potentially the most destructive of all volcanic phenomena, due to the large distances that some types are capable of travelling and to their high temperature. Serious loss of life has been caused by several small historic pyroclastic flows. Small historic flows have been observed to move up to about 20 km from vent at speeds as high as 60 m s^{-1} (J. G. Moore & Melson 1969, D. K. Davies *et al.* 1978a). However, field studies of older Quaternary deposits suggest that the larger flows (forming ignimbrites) have travelled distances of >100 km from vent, and theoretical analysis based on measurements of the heights of mountains climbed by pyroclastic flows suggests that average speeds of >100 m s^{-1} are common (Ch. 7).

Pyroclastic flows are generated by a number of different mechanisms (Fig. 5.11). From what we understand of observed modern eruptions, these can be split initially into two main types:

lava-dome or lava-flow collapse
eruption column collapse

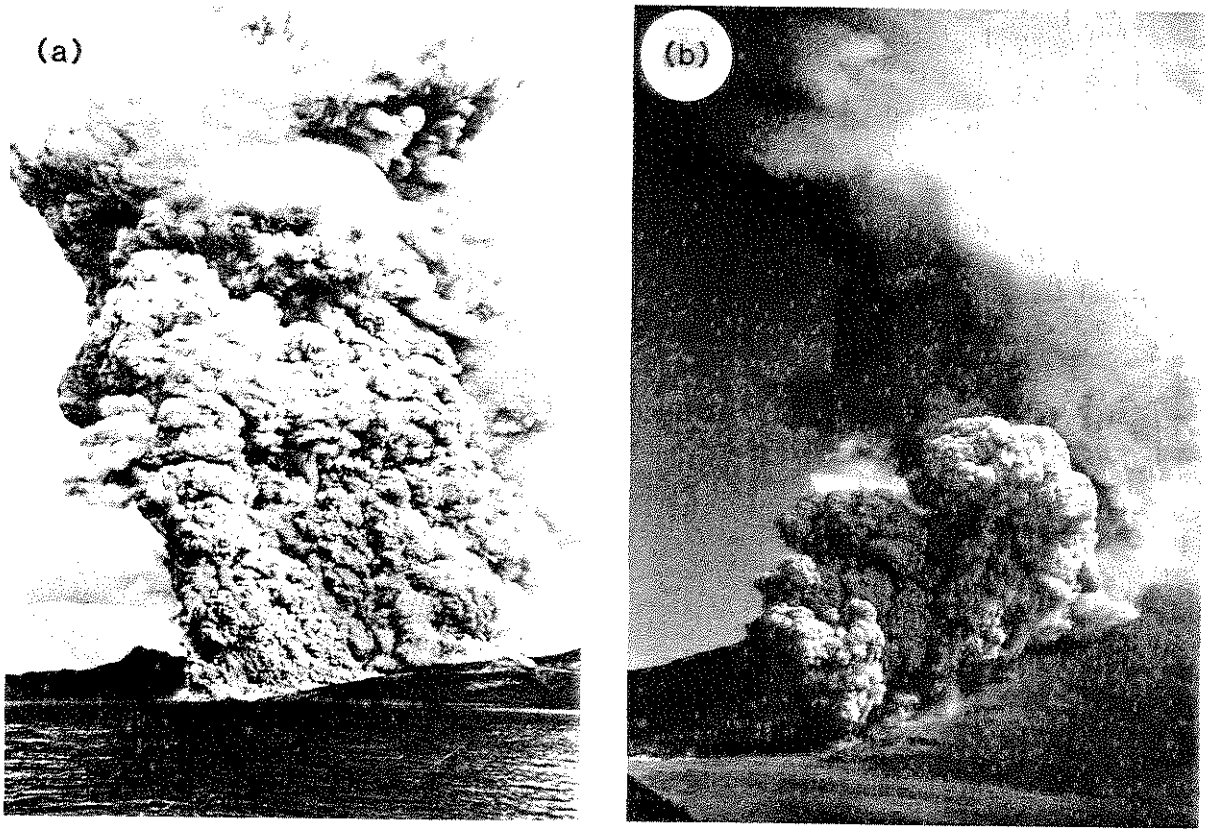

Figure 5.10 Two pyroclastic flows. (a) Towering ash cloud 4000 m above a pyroclastic flow moving down the Rivière Blanche from Mt Pelée during an eruption in December 1902 (after La Croix 1904). (b) Pumiceous pyroclastic flow erupted on 7 August at Mt St Helens in 1980. This flow travelled at speeds in excess of 30 m s^{-1}. (After P. W. Lipman in Rowley *et al.* 1981.)

(a) Gravitational dome collapse

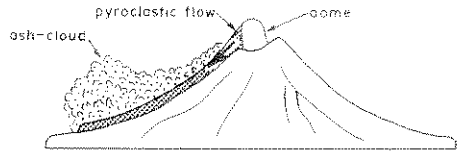

(b) Explosive dome collapse

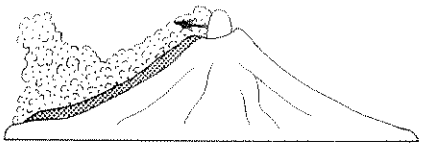

(c) Landslide triggering explosive collapse of cryptodome

(d) Discrete explosions interrupted column collapse

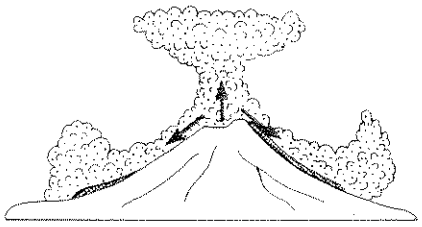

(e) Continuous gas streaming interrupted column collapse

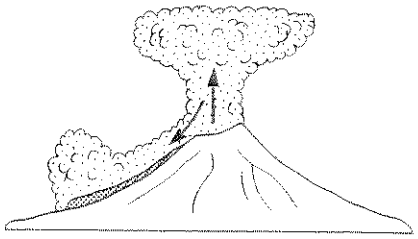

(f) Upwelling at vent "instantaneous collapse"

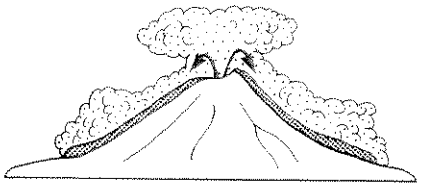

(g) Vertical explosion from dome eruption column collapse

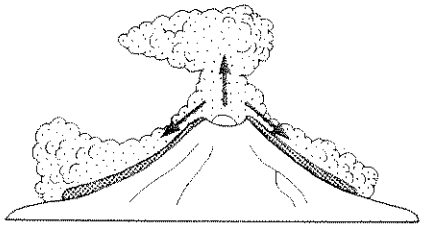

(h) Continuous eruption column collapse

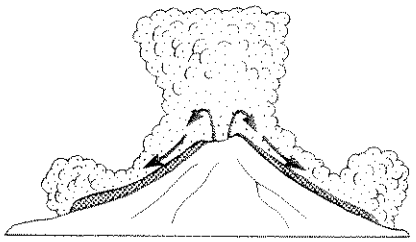

Figure 5.11 Mechanisms generating pyroclastic flows. The pyroclastic flow proper is a high particle concentration underflow. The ash cloud gives rise to other deposits (Fig. 5.13).

5.4.1 LAVA-DOME OR LAVA-FLOW COLLAPSE

This mechanism typically operates on steep-sided andesitic volcanic cones, but also occurs during the eruption of silicic domes not related to major edifices. Fragmental flows of broken lava are generated when an unstable, actively growing lava-dome or lava-flow collapses from the summit or high on the flanks of the volcano. Collapse may be simply gravitational (which is not strictly pyroclastic), or could be an explosively directed blast (Figs 5.11a & b). However, pressure release within a dome due to an initial gravitational collapse could lead to explosive collapse so, in some cases, both processes may have occurred. Explosions could also be triggered by contact of the growing dome with ground water. Such an eruption could therefore be considered to be phreatomagmatic. This also leads to the possibility that phreatic explosions could generate pyroclastic flows containing no juvenile fragments (e.g. Sheridan 1980). It is therefore important to realise that different processes may have occurred at about the same time, and the relative importance of each is, perhaps, difficult to distinguish.

These types of pyroclastic flow we will term **block and ash flows**, but other terms in use are **lava debris flows**, **hot avalanche deposits** (P. W. Francis *et al.* 1974) and **nuées ardentes** (see Ch. 12). Block and ash-flows are small-volume pyroclastic flows, and even the deposits of many separate flows or flow units accumulated during the same eruption typically have volumes <1 km^3.

Examples of historic eruptions during which explosive lava-dome or lava-flow collapse was observed are the eruptions of Mt Pelée, Martinique in 1902 and 1929–32 (La Croix 1904, Perret 1937), Merapi, Indonesia in 1942–3 (van Bemmelen 1949), the eruptions of Hibok-Hibok, Philippines (1951) (MacDonald & Alcaraz 1956), Mt Lamington, Papua New Guinea (1951) (G. A. Taylor 1958), and Santiaguito, Guatemala (1973) (Rose *et al.* 1978). Historic examples where simple gravitational collapse of a dome occurred are the eruptions of Merapi in 1930 and 1942–3 (Neumann van Padang 1933, van Bemmelen 1949) and Santiaguito in 1967 (Stoiber & Rose 1969).

Here we must also ask whether the 1980 eruption of Mt St Helens should be considered to be another example of an explosive dome collapse. The explosive eruption of 18 May was initiated when a giant landslide, triggered by an earthquake, released the confining pressure on a rising dacitic dome (or cryptodome; Ch. 4) which was intruded high into the north flank of the volcano (Christiansen & Peterson 1981). A large rockslide avalanched, and was quickly followed by an explosive directed blast (Fig. 5.11c; also see Fig. 10.6). Explosions were generated by flashing of superheated ground water as well as release of magmatic gases when the dome and its hydrothermal system were exposed and depressurised by the landslide. The avalanche formed a relatively '*hot* and *dry*' volcaniclastic debris flow consisting almost entirely of older volcanic rocks with little juvenile material (<1%; Voight *et al.* 1981). At the time of emplacement much of the deposit was as hot as 100°C, and it is perhaps debatable whether it should be termed a pyroclastic flow deposit. What to call the deposit of the blast has again been somewhat debatable, but it has been widely regarded as a pyroclastic surge (Section 5.6) and, more recently, as a pyroclastic flow (Section 7.12). Although the eruption was an explosive dome collapse, the eruption and its deposits seem to be more complicated than those generating the block and ash flows that we have described previously. The events at Mt St Helens also triggered a nine hour dacitic plinian eruption with pumice flows forming an ignimbrite (Section 5.5).

There may have been several historic eruptions in which there has been a collapse of a sector of the volcano similar to the one observed at Mt St Helens. The eruption of Bezymianny in 1956 (Gorshkov 1959) produced a directed blast and pyroclastic flows (as well as a very high eruption column dispersing air-fall ash; Fig. 5.9), and is sometimes given as an example of explosive dome collapse (e.g. J. V. Wright *et al.* 1980). The '*agglomerate flows*' of Gorshkov (1959) may have been a similar volcaniclastic debris flow to the Mt St Helens rockslide avalanche, containing a large proportion of non-juvenile material, judging from the horseshoe-shaped amphitheatre that was left

after the eruption. However, these deposits also had a substantial amount of juvenile material and were 'identifiable' as pyroclastic flow deposits. Other eruptions, at Bandai-san, Japan in 1888 (Nakamura 1978), and Shevefuch, Kamchatka in 1964 (Gorshkov & Dubik 1970), seem to have produced similar chaotic deposits, but made entirely or almost entirely from non-juvenile fragments. Therefore, there could be a broad spectrum of deposits produced by collapses of this kind, ranging from recognisable explosively generated block- and ash-flow deposits (or even other types of pyroclastic flow deposit), to volcaniclastic debris flow deposits with no (or very little) juvenile material. Distinguishing such deposits, which lack a high proportion of juvenile fragments, from those formed by epiclastic debris flows is going to be, even in the late Quaternary record, very difficult. Criteria by which to identify such hot, dry volcaniclastic debris-flow deposits have been discussed by Ui (1983) and Siebert (1984).

5.4.2 ERUPTION COLUMN COLLAPSE

In this case, the effective density of a vertical ash-laden eruption column is greater than that of the atmosphere, and gravitational collapse occurs, generating a pyroclastic flow. All of the historic examples of this type have again produced small-volume pyroclastic flow deposits. Many of these were probably formed by interrupted, partial column collapse events. Observations suggest that such small collapses occur when either a short explosion ejects a dense slug of pyroclastic fragments to an altitude of a few hundred metres, part of which then falls back (Fig. 5.11d), or as overloaded parts of a more maintained vertical column produced by continuous gas streaming, collapse (Fig. 5.11e). Both types of collapse event are common during vulcanian activity, but pyroclastic flows are not always generated in such eruptions, and air-fall deposits may be the sole products (Ch. 6). Observed historic eruptions during which this type of pyroclastic flow formed are Mt Lamington (1951) (G. A. Taylor 1958), Mayon, Philippines (1968) (J. G. Moore & Melson 1969), Fuego (1974) (D. K. Davies *et al.* 1978a)

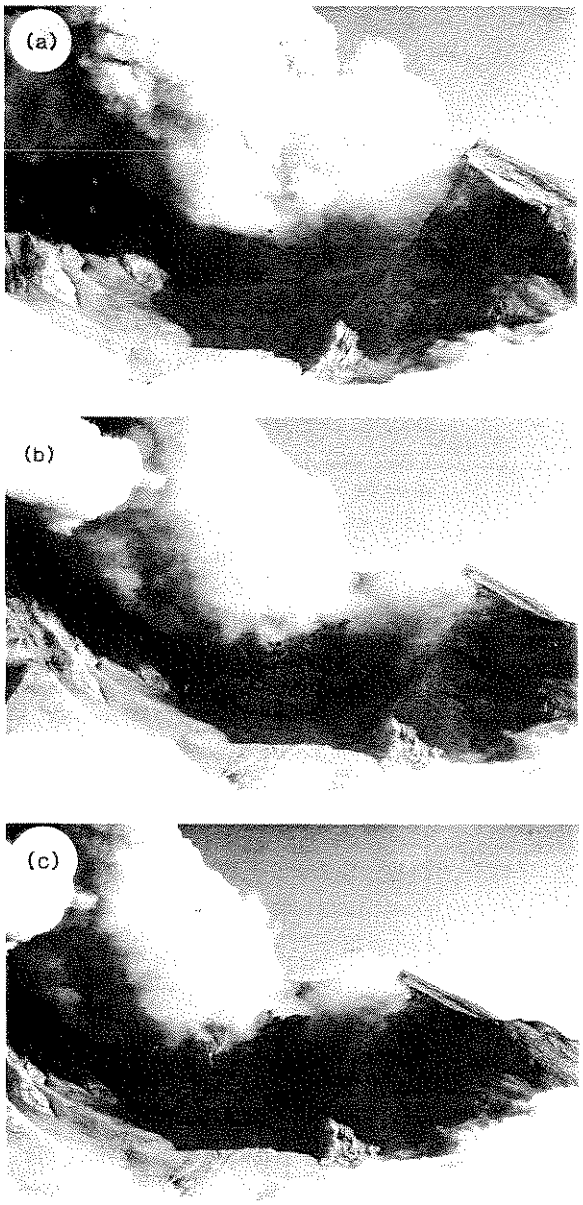

and Ngauruhoe (1975) (Nairn & Self 1978). All produced scoria flows or scoria and ash flows. These types of pyroclastic flows have also been called nuées ardentes and pyroclastic avalanches (Nairn & Self 1978).

Some older eyewitness accounts recorded by Wolf (1878) of the eruption of Cotopaxi, Ecuador, in 1877 suggest that another mechanism should be

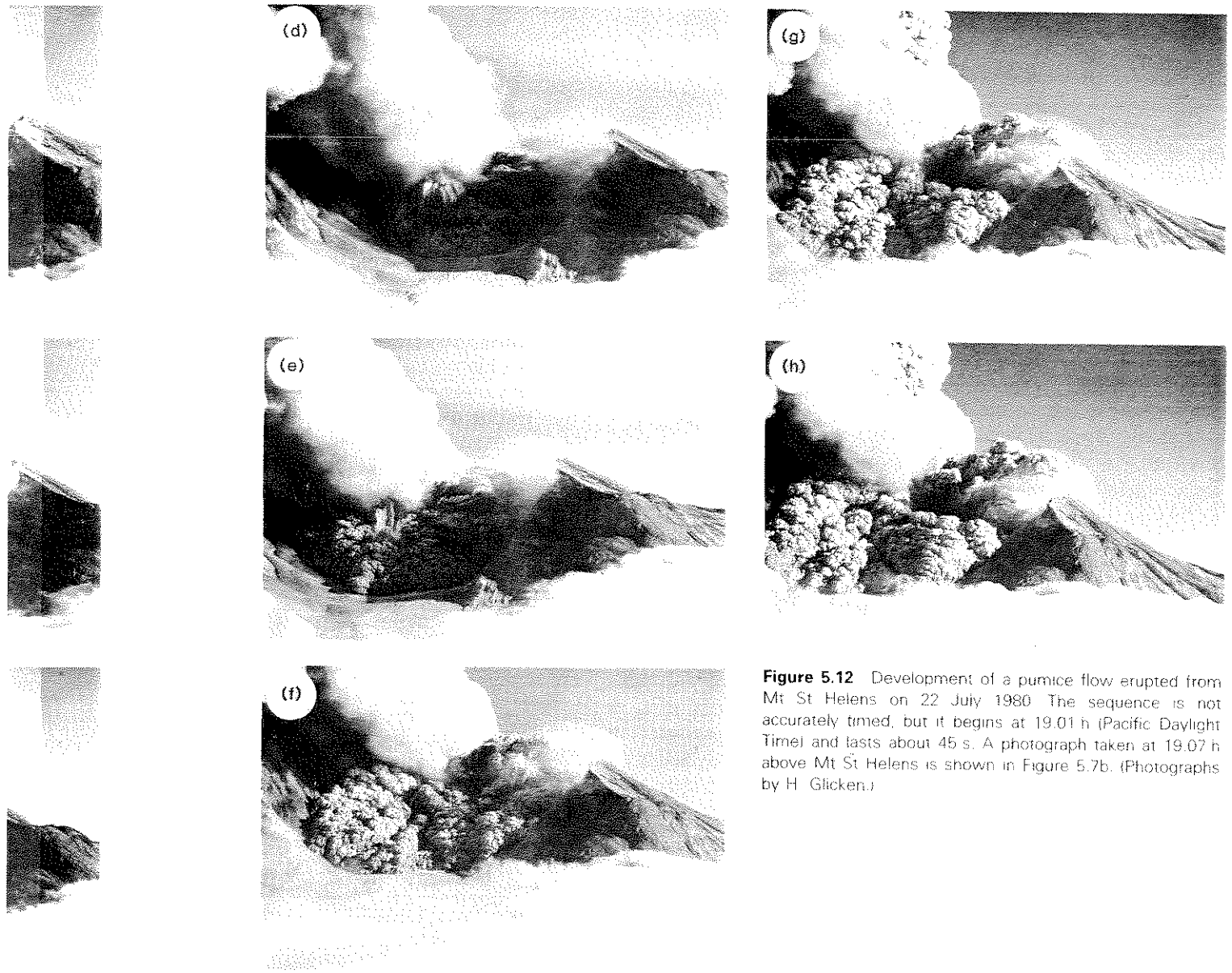

Figure 5.12 Development of a pumice flow erupted from Mt St Helens on 22 July 1980. The sequence is not accurately timed, but it begins at 19.01 h (Pacific Daylight Time) and lasts about 45 s. A photograph taken at 19.07 h above Mt St Helens is shown in Figure 5.7b. (Photographs by H. Glicken.)

1978). All
ash flows.
also been
avalanches

corded by
Ecuador,
should be

considered for the eruption of scoria flows. Many of the local people who had observed the eruption described it as 'a pan of rice boiling over'. This suggests that these pyroclastic flows may have originated directly out of the vent, and formed without the collapse of an eruption column, or from a column so dense that it only rose a small height above the vent and instantaneously collapsed and 'bubbled over' (Fig. 5.11f).

It thus seems likely that so-called 'column collapse' that sources pyroclastic flows can take different forms. These include variations ranging from discrete column collapse of high, well maintained columns to partial collapse events from the margins of an unstable, but established, column, to discrete collapse followed by essentially continuous

fountaining of pyroclastic debris, to a more passive boiling over, directly out of the vent.

It is now also thought that block and ash flows may be produced by collapse of eruption columns (Fig. 5.11g). Fisher and Heiken (1982) suggested that some of the explosions in the early stages of the Mt Pelée 1902 eruption were vertical rather than directed laterally. Collapse of a vertical column, or a slug of lava debris out of it, generated block and ash flows rather than a directed blast. It was eruptions of this type that occurred on 8 and 20 May 1902, and led to the destruction of St Pierre, and the death of 30 000 people.

The deposits of pumiceous pyroclastic flows are termed **ignimbrite**, and some of these can be very large volume deposits (>1000 km^3). Few ignimbrites have been erupted this century. Those that have are only small-volume deposits (Ch. 8), and there is little observational information for these. The generally known examples are the Valley of Ten Thousand Smokes ignimbrite erupted from Katmai, Alaska, in 1912 (C. N. Fenner 1920, Curtis 1968), those formed during the eruptions of Komagatake, Japan, in 1929 (Aramaki & Yamasaki 1963) and those from Mt St Helens in 1980. Two notable, and larger, ignimbrite-forming eruptions occurred last century: Krakatau, west of Java, in 1883 (Self *et al.* 1981) and Tambora, also in Indonesia, in 1815 (van Bemmelen 1949, Self *et al.* 1984).

Small-volume pumice flows, like scoria flows, are perhaps in many cases generated by interrupted column collapse. Nobody has yet observed a large-volume ignimbrite-forming eruption, although as early as 1960, R. L. Smith (1960a) suggested that they could be formed by an eruption column collapse mechanism, but on a larger scale. Sparks and L. Wilson (1976) and Sparks *et al.* (1978) presented a theoretical model for the formation of ignimbrites based on the continuous gravitational collapse of a plinian eruption column (Fig. 5.11h). This models helps to explain many features of ignimbrites (Chs 7 & 8), and has since become popular among workers in this field. Continuous collapse of plinian eruption columns from heights of several kilometres could account for the large volume and wide distribution of some ignimbrites. The model is also appealing because it explains why many ignimbrites are underlain by plinian pyroclastic fall deposits (Fig. 5.6b, Chs 6 & 8).

However, observations of the Mt St Helens 1980 eruption suggest that many of the pumiceous pyroclastic flows, which under our definition form ignimbrite, were not generated by collapse of a high eruption column (Rowley *et al.* 1981), but from low columns. Many pumice flows seemed to spread out from bulbous inflated masses of pyroclasts as they upwelled a short distance above the vent. The sequence of photographs in Figure 5.12 of activity on 22 July illustrate this particularly well, showing the development and instantaneous collapse of a fountain about 500 m high. Descriptions such as a 'pot boiling over' were given (Rowley *et al.* 1981), and there are obvious similarities to the eyewitness descriptions given of the Cotopaxi eruption in 1877. During other periods of activity, partial gravitational collapse of the margins of maintained columns was observed. None of the Mt St Helens pumice flows travelled very far, and all are minor in volume.

These new observations suggest that column collapse as the only mechanism for the generation of ignimbrites may have been overemphasised in recent years, as suggested above. In some instances 'spluttering' or 'frothing' at the vent may be more important. We will develop and expand these ideas on eruption mechanisms of ignimbrites through Chapters 6 and 8.

5.5 Pyroclastic flow deposits: types and description

Most pyroclastic flow deposits are composed of more than one flow unit. Each flow unit is usually regarded as the deposit of a single pyroclastic flow (Fig. 5.13), one of perhaps several or many generated during the course of the same eruption (Sparks *et al.* 1973, Sparks 1976). However, it is certainly possible that as a pyroclastic flow advances it could split into several subflows (R. L. Smith 1960a; and observed at Mt St Helens), each represented in the field by a discrete depositional flow unit. In the field pyroclastic flow units may be

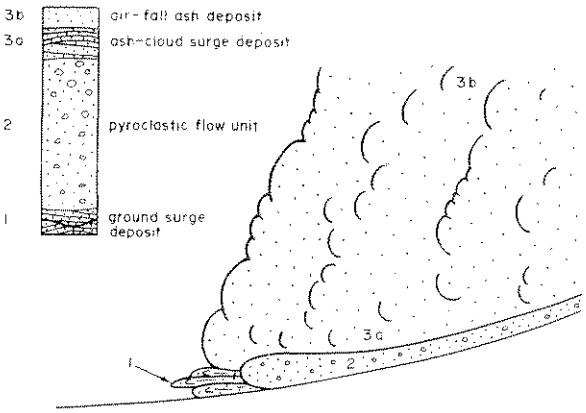

Figure 5.13 Schematic diagram showing the structure and idealised deposits of one pyroclastic flow

seen to be stacked on top of each other, or be separated by other pyroclastic layers (fall or surge deposits) or reworked epiclastic deposits.

From the foregoing discussion on pyroclastic flow forming eruptions, it appears that three main types of pyroclastic flow deposit are recognised in modern volcanic successions (Figs 5.14–16):

block- and ash-flow deposits
scoria-flow deposits
pumice-flow deposits or ignimbrite

5.5.1 BLOCK- AND ASH-FLOW DEPOSITS

These are topographically controlled, unsorted deposits having an ash matrix and containing large generally non-vesicular, cognate lithic blocks which can exceed 5 m in diameter (Figs 5.14a & 15a). Some of these blocks contain radially arranged cooling joints which show they were emplaced as hot blocks (Fig. 5.15b). Clasts should be all of the same magma type, and therefore the deposits should be, or almost be, monolithologic. Individual flow units are reversely graded in many examples (Figs 5.14a & 15a). They may contain gas segregation pipes (Figs 5.15c & d), although these are not found too commonly in block and ash deposits (Ch. 7), and carbonised wood. Surface manifestations include the presence of levées, steep flow fronts and the presence of large surface blocks, all of which again indicate a high yield strength during flow. No welded examples are known to us, although Sparks (*pers. comm.*) reports one on the southern flanks of Mt Pelée.

Homogeneous clast composition, hot blocks and gas segregation pipes are the field criteria for distinguishing these pyroclastic flow deposits from types of sedimentary debris deposits such as rock avalanches and debris flows (Ch. 10).

5.5.2 SCORIA-FLOW DEPOSITS

These are topographically controlled, unsorted deposits with variable amounts of basaltic to andesitic ash, vesicular lapilli and scoriaceous ropy surfaced clasts up to 1 m in diameter (Figs 5.14b & 5.15d–f). In some circumstances they may contain large non-vesicular cognate lithic clasts (Fig. 5.15f). Reverse grading of larger clasts within flow units is common, and fine-grained basal layers are sometimes found at the bottom of flow units. Gas segregation pipes and carbonised wood may also be present. The presence of levées, channels and steep flow-fronts indicates a high yield strength during flow. Again, we know of no welded examples.

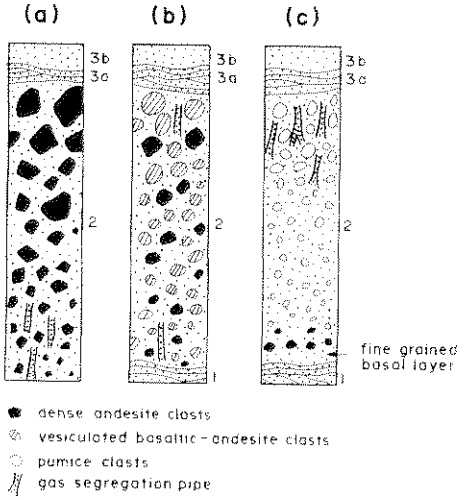

Figure 5.14 Idealised sections of the three main types of pyroclastic flow deposit and associated layers deposited by the mechanisms suggested in Figure 5.13. (a) Block and ash-flow deposit. (b) Scoria-flow deposit. (c) Pumice-flow deposit or ignimbrite

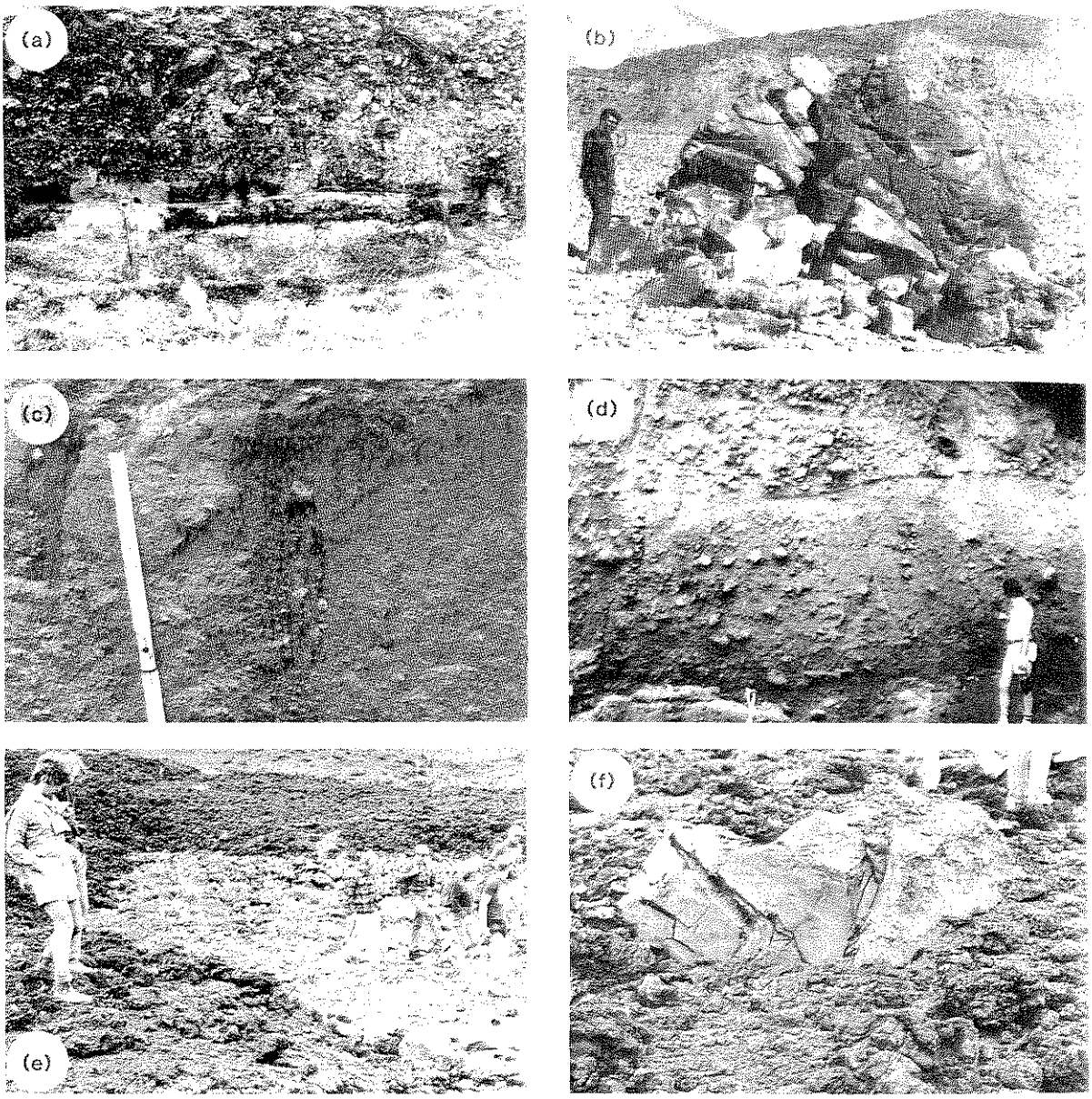

Figure 5.15 Block- and ash-flow and scoria-flow deposits. (a) Reversely graded block and ash-flow deposit, formed by collapse of a rhyolitic lava flow. This was erupted towards the end of the 700 years BP Kaharoa eruption of the Tarawera volcanic centre, New Zealand. Top of spade handle is base of block and ash-flow deposit, other layers are earlier co-eruptive products. (b) Hot block in block and ash-flow deposit, San Pedro volcano, northern Chile (after P. W. Francis *et al.* 1974). (c) Gas segregation pipes in the 1902 block and ash flow deposits erupted from Mt Pelee (after Fisher & Heiken 1982). (d) Scoria flow deposit erupted from Mt Misery volcano, St Kitts, Lesser Antilles. Note the concentration zones of scoria which seem to be associated with flow unit boundaries and coarser-grained pipes which have been emphasised by rain washing. Arrow points to a carbonised log from which a ^{14}C age of 2860 years BP was obtained (photograph by M. J. Rooboll). (e) and (f) The scoria flow deposits (dark) erupted in 1975 at Mt Ngauruhoe, New Zealand. Note thin lobate flow front and dense juvenile fragments with more scoriaceous clasts.

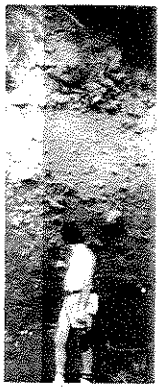

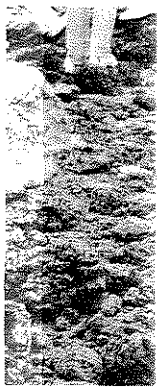

osit, formed by
f the Tarawera
rlier co-eruptive
et al. 1974). (c)
982). (d) Scoria
which seem to
washing. Arrow
ket and (f) The
dense juvenile

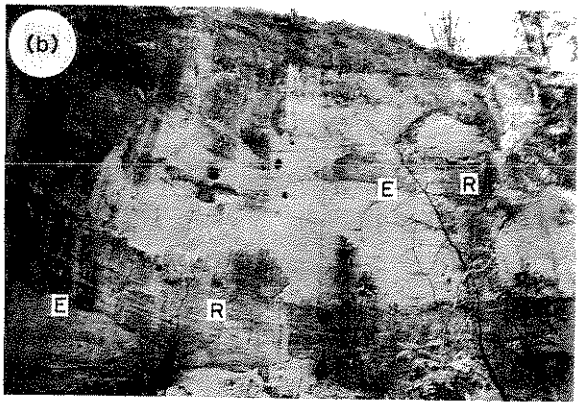

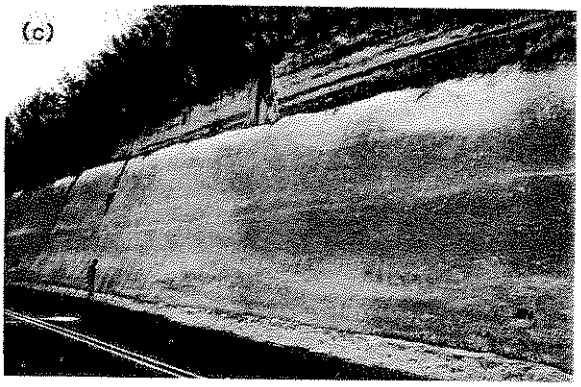

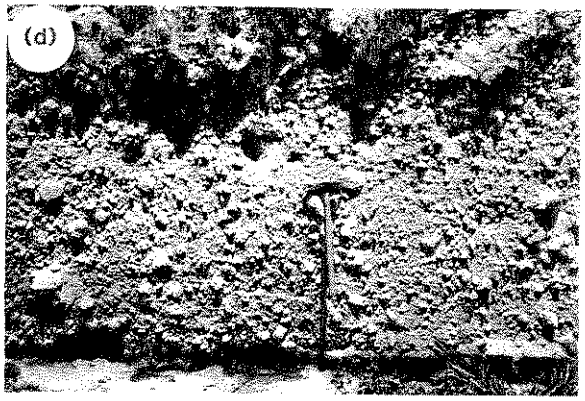

Figure 5.16 Some general features of pumice-flow deposits. All of the photographs are from non-welded ignimbrites or non-welded zones of welded ignimbrites. (a) Stacked thin flow units of the Rio Caliente ignimbrite, Mexico. Flow unit boundaries are picked out by fine-grained basal layers (after J. V. Wright 1981). (b) Flow units of the Rio Caliente ignimbrite interbedded with fluviatile reworked pumice (R) and erosion surfaces (E); arrow points to two flow units filling in small channels cut into the succession. No soils are present, and field evidence elsewhere shows that these erosional events must have been local and short-lived, and occurred during the same eruption. Height of cliff section is about 16 m (after J. V. Wright 1981). (c) Thick, massive flow unit of the Oruanui ignimbrite in New Zealand, which is poorly sorted and texturally very homogeneous throughout the thickness seen (horizontal lines are bulldozer scrapings). (d) Coarse, poorly sorted pumice-flow deposit on St Lucia, Lesser Antilles. (e) Close-up showing poor sorting in an ignimbrite. This is from a flow unit of the Acatlan ignimbrite, Mexico. Dark clasts are lithics.

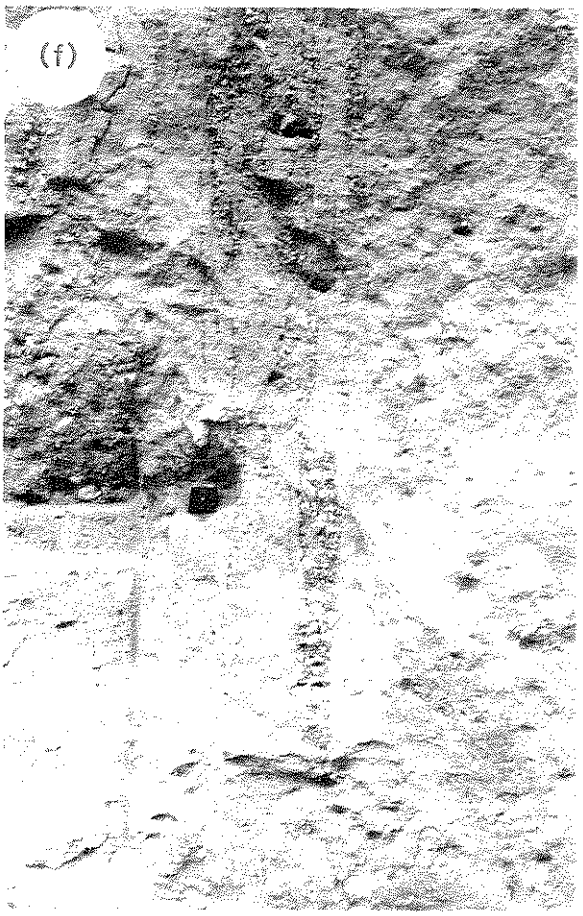

Figure 5.16 continued (f) 'Fossil fumaroles': crystal and lithic enriched gas segregation pipes in the Taupo ignimbrite, New Zealand (photograph by C. J. N. Wilson)

5.5.3 PUMICE-FLOW DEPOSITS OR IGNIMBRITES

Ignimbrites are typically poorly sorted, massive deposits containing variable amounts of ash, rounded pumice lapilli and blocks occasionally up to 1 m in diameter (Figs 5.14c & 16). Within flow units, larger pumice fragments can be reversely graded, while lithic clasts can show normal grading. However, ungraded flow units are as common. A fine-grained basal layer is usually found at the bottom of flow units (Fig. 5.16a). The coarser, smaller-volume deposits usually form valley infills, while the larger-volume deposits may form large ignimbrite sheets that bury all but high topographic features. Sometimes they may show one or more zones of welding (Ch. 8). Their common salmon-pink colour, the presence of carbonised wood and a thermal remanent magnetisation are all ways of distinguishing non-welded ignimbrites from the deposits of pumiceous mud flows. Also, ignimbrites sometimes contain gas segregation pipes (Fig. 5.16f).

5.6 Origins of pyroclastic surges

It is now apparent that dilute, low particle concentration, turbulent, pyroclastic surges can be generated in many different ways. Volcanic base surges, first described from the phreatomagmatic eruptions of Taal volcano, Philippines, in 1965 by J. G. Moore *et al.* (1966) and J. G. Moore (1967), are *only one type* of pyroclastic surge. Pyroclastic surges are known to form in three situations, associated with:

phreatomagmatic and phreatic eruptions
pyroclastic flows
pyroclastic falls

5.6.1 SURGES ASSOCIATED WITH PHREATOMAGMATIC AND PHREATIC ERUPTIONS

These eruptions can generate a base surge which is a collar-like, low cloud expanding radially in all directions from the locus of a phreatomagmatic or phreatic explosion and/or by the collapse of the phreatomagmatic or phreatic eruption column (Figs 5.17 & 18). The term 'base surge' was originally applied to the radially outward moving basal clouds observed and photographed in nuclear explosions (Fig. 5.17), to which J. G. Moore (1967) likened similar features observed during the Taal 1965 eruptions, and some other observed historic eruptions.

The eruption of Taal on 28–30 September 1965 took place when water gained access to rising basaltic magma on the southwest side of Volcano Island, Lake Taal (J. G. Moore *et al.* 1966, J. G.

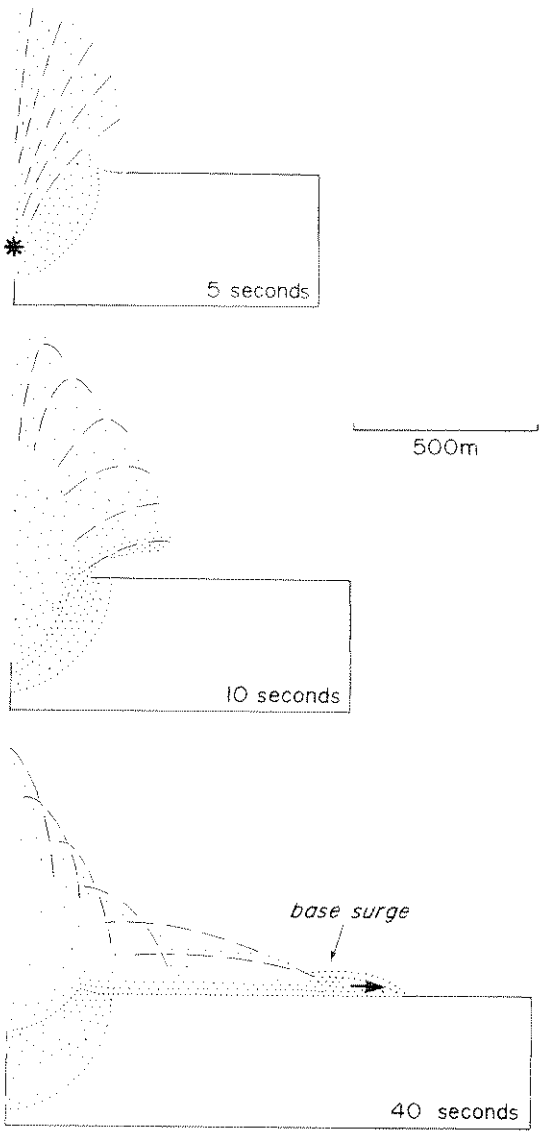

Figure 5.17 Sequential diagram showing formation of a base surge after an underground explosion equivalent to 100 kilotons of chemical explosives. (After J. G. Moore 1967.)

Moore 1967; Fig. 5.19). Explosions produced a series of base surges (Fig. 5.19) which spread out radially with 'hurricane velocity', causing extensive damage and loss of life. These debris-laden clouds obliterated and shattered all trees within 1 km of the explosion centre, and sandblasted objects up to 8 km away. Initially, velocities may have been as high as 100 m s^{-1} (J. G. Moore 1967).

Base surges result from the explosive interaction of magma and water and are probably in many cases *'cold and wet'* (Ch. 7). In the entire area affected by base surges from the Taal 1965 eruption, no evidence of charred wood was found on surviving trees or in the deposits. In the zone where ash was plastered on to objects (Fig. 5.19b) the ash must have been mixed with water rather than steam to have been so sticky, and surges would have had temperatures below 100°C (J. G. Moore 1967). However, some phreatomagmatic eruptions have produced hot pyroclastic surges. During the phreatomagmatic eruptions forming the Ukinrek maars, Alaska, in 1977 (e.g. Fig. 5.18c), pyroclastic surges charred tree branches and trunks (Self *et al.* 1980). As discussed in Chapter 3, Sheridan and Wohletz (1981) suggested that there is a natural division between wet and dry base surges, depending on the water : magma mass ratio in phreatomagmatic explosions (Fig. 3.9). With a low water : magma mass ratio *'dry and hot'* base surges may be produced.

Base surges are commonly associated with the formation of small volcanic craters, called variously maars, tuff rings and tuff cones (Ch. 13). These are common features in areas of basaltic volcanism, and without the interaction of ground or surface water or sea water, the basaltic magma would have erupted to form scoria cones and lava flows. There have been a number of eruptions of this type in the 20th century. For descriptions and analysis of this type of activity, the reader is referred to Moore (1967) and Waters and Fisher (1971), who show spectacular photographs of the eruptions of Capelinhos in 1957–8 in the Azores (Figs 5.18a & b) and Taal, Philippines, in 1965–6, and the papers by Kienle *et al.* (1980) and Self *et al.* (1980) describing the formation of the Ukinrek maars, Alaska (Fig. 5.18c). Maars and maar-like constructional landforms can be formed by eruptions of other magma types, including carbonatitic, phonolitic and rhyolitic compositions. For good descriptions of the base-surge deposits associated with prehistoric phonolitic and rhyolitic eruptions of this type see Schmincke *et al.* (1973) and Sheridan and Updike (1975), respectively.

Base surges are also known to be erupted from major volcanoes. They should be common products

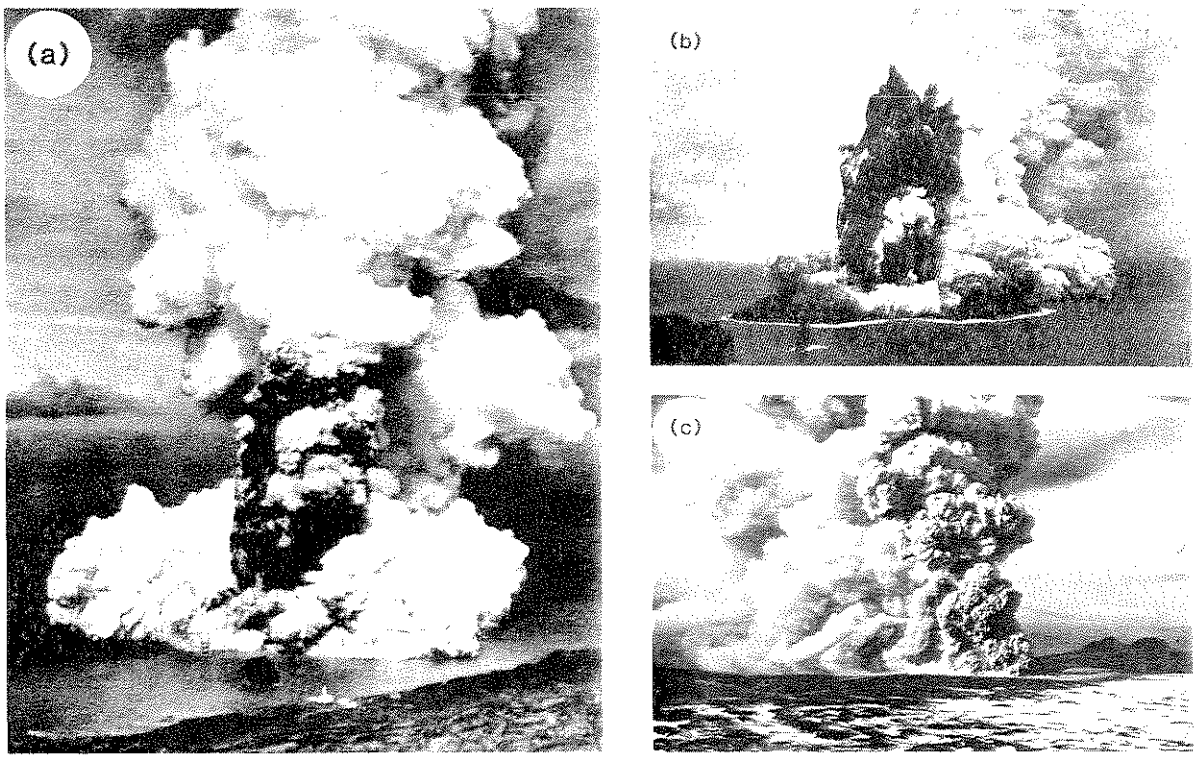

Figure 5.18 Phreatomagmatic eruptions producing base surges. (a) At Capelinhos in October 1957. Height of vertical column to top of photograph is about 2200 m. US Air Force photograph (after J. G. Moore 1967). (b) Capelinhos in September 1957. Steam has blown downwind to expose a dense debris-laden central column collapsing to feed a base surge. On the right-hand side of the photograph the surge is moving across the ocean surface (after Waters & Fisher 1971). (c) East Ukinrek maar in 1977. Note chevron shape of base surge cloud (moving to the left) which in this case was directed by lows in the maar rim and shallow valleys (after J. Faro in Kienle *et al.* 1980).

of andesitic stratovolcanoes with crater lakes, and other volcanoes with caldera lakes. Phreatic and phreatomagmatic eruptions from the crater lake of Ruapehu volcano, New Zealand, have been common this century, and base surges were observed in the eruption of April 1975 (Nairn *et al.* 1979). The 1979 eruption of Soufrière, St Vincent, which was through a crater lake, also produced base surges (Shepherd & Sigurdsson 1982). The Quill stratovolcano on St Eustatius, also in the Lesser Antilles, has a long history of phreatomagmatic activity, and base-surge deposits form an important part of the pyroclastic succession found in its ring plain. These vary from basaltic andesite to rhyolite in composition, and were produced by a number of eruptions over the past ~30 000 years as the volcano emerged from the sea and grew to its present form (Roobol, Smith & Wright *unpub. data*). The rhyolitic base-surge deposits form part of a thicker pyroclastic sequence generated during an ignimbrite-forming eruption. Rhyolitic base-surge deposits are also known in association with phreatoplinian phases of the Askja, Iceland, 1875 eruption and the Minoan (1470 BC) eruption of Santorini (Self & Sparks 1978; Ch. 6). Phonolitic base surges also were generated late during the AD 79 eruption of Vesuvius, when large amounts of water from a deep aquifer under the volcano gained access to the magma chamber. The deposits are associated with phreatoplinian air-fall layers (Sheridan *et al.* 1981; Ch. 6).

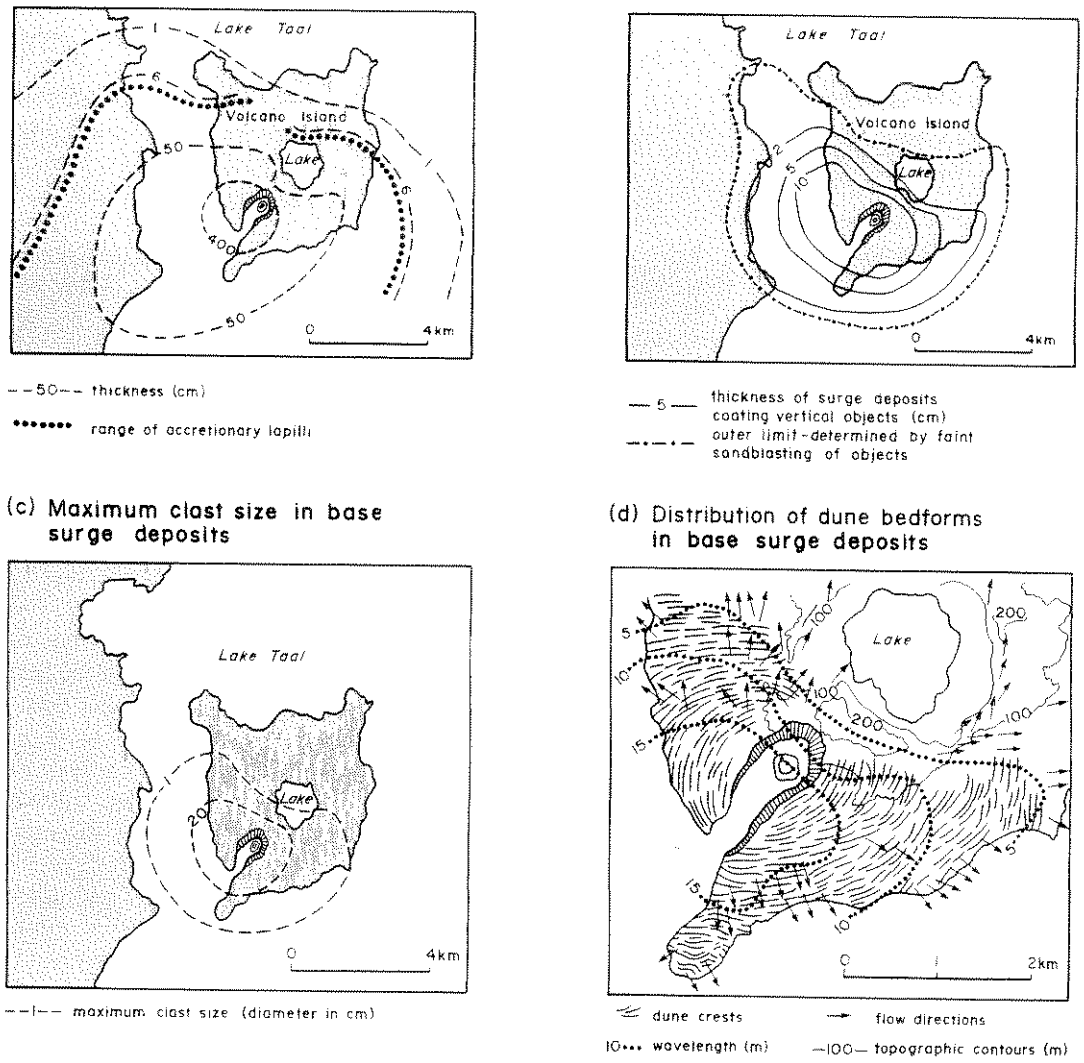

Figure 5.19 General distributional characteristics of the deposits of the 1965 eruption of Taal in the Philippines. Flow directions of major base surge movement in (d) were measured in the field from the sand blasting, tilting and coating of trees and houses. (After J. G. Moore 1967.)

5.6.2 SURGES ASSOCIATED WITH FLOWS

Thin, stratified pumice and ash deposits are often found associated with pyroclastic flow deposits of various kinds. When associated with the bases of flow units, they are called **ground surges**, and when associated with the tops they are called **ash-cloud surges**. These types have different mechanisms of generation. Compared with base surges they can be considered to be hot and dry.

The term 'ground surge' was coined by Sparks and Walker (1973), but it was used by these authors to mean any type of pyroclastic surge. More recently the term has become used just for those surges found at the bases of pyroclastic flow units, or associated with some fall deposits (Section 5.6.3;

Fisher 1979, J. V. Wright *et al.* 1980). Ground surges are thought to be the same as the 'ash hurricanes' described by G. A. Taylor (1958) from the 1951 Mt Lamington eruption. Taylor observed these to form at the same time as high concentration pyroclastic flows (or his 'ponderous ash flow nuees') directly from the crater without an accompanying vertical eruption column, or from collapsing eruption columns (Fisher 1979).

Ground surges are envisaged as precursors to dense, high concentration pyroclastic flows, preceding their flow-fronts. There are a number of ways in which they can be generated:

(a) from a directed low concentration blast,
(b) out of the head of a moving pyroclastic flow or
(c) by earlier, smaller collapses of the margins of a maintained vertical eruption column.

The concept of a low concentration blast preceding the main part of a pyroclastic flow stems largely from early ideas on understanding the 8 May 1902 eruption of Mt Pelée, which was thought to have been a directed blast. We have already discussed this eruption, and how it is now thought to have generated block and ash flows by collapse of an eruption column. Fisher *et al.* (1980) and Fisher and Heiken (1982) suggested that St Pierre was destroyed by an ash-cloud surge, although G. P. L. Walker and McBroome (1983) suggested that it was by a violent pyroclastic flow (Ch. 7). Several historic block- and ash-flow deposits produced by explosive lava-dome collapse have obvious surge deposits associated with them, but again some of these could be ash-cloud surge deposits. However, Rose *et al.* (1977) described a ground surge produced by explosive collapse directed out of the lava front at Santiaguito in September 1973, and because the surge does not mantle the associated block- and ash-flow deposit, they suggest that it probably preceded it. The initial explosion of Mt St Helens was an obvious directed blast, and its effect on the forest in its path is well known. The deposits from the initial explosion certainly show some characteristics of a surge deposit, as we have alluded to previously, and this is how they have been described by J. G. Moore and Sisson (1981) and Hickson *et al.* (1982). However, the stratigraphy is more complicated than that of normal ground-surge deposits, and Hoblitt *et al.* (1981) have drawn attention to this. G. P. L. Walker (1983) suggested that the blast was a high concentration pyroclastic flow emplaced at very high velocities, like some violent ignimbrites (Chs 7 & 8). Like the Mt Pelée event, this event and its deposits are the source of much debate. Pumice flows forming ignimbrite did not begin to erupt for another four hours after the initial explosion at Mt St Helens.

Studies by C. J. N. Wilson (1980, 1981, 1984) and C. J. N. Wilson and Walker (1982) suggest that the flow-heads of some pyroclastic flows (especially pumice flows) may ingest large volumes of air, and may be inflated and highly fluidised (Chs 7 & 8). At the front of the moving flow, basal friction will cause an overhang which will act as a funnel for air, in much the same way as a subaqueous mass flow incorporates water (Allen 1971, Simpson 1972). Cold air when heated would rapidly expand, and surges of highly fluidised pyroclasts would be jetted out of the head and upper parts of the flow front (Fig. 5.13; Ch. 7); material ejected at higher positions on the flow-front would contribute to the ash cloud. This could also be another mechanism for generating turbulent, low concentration surges continually advancing in front of some pyroclastic flows. The escaping gas and ash gives the flow-head its 'billowing' or 'sprouting' appearance, as seen, for example, by Perret (1937) in some Mt Pelée pyroclastic flows erupted during 1929–32. This type of jetting of material from the flow-head explains some other facies associated with ignimbrites, and these will be discussed further in Chapter 7.

The third mechanism we can envisage for the generation of ground surges is by repeated minor collapse of a maintained eruption column before major ignimbrite-forming collapse. This could also apply for some ignimbrite-forming eruptions, and Fisher (1979) suggested such a model. Turbulent mixing and intake of cold air at the margins of the eruption column could overload parts of it, and small-scale collapse could generate precursor surges.

More recently, however, G. P. L. Walker *et al.*

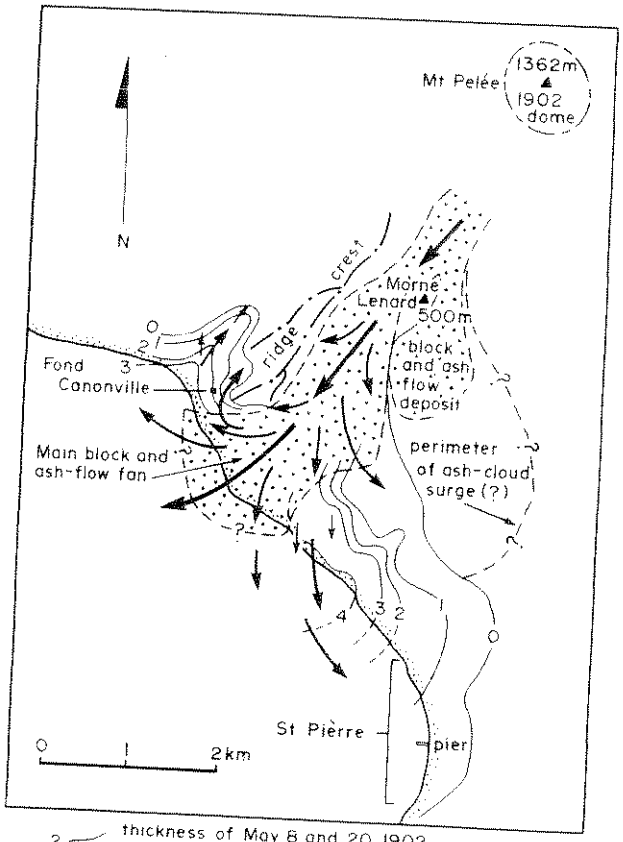

Figure 5.20 Distribution of the block and ash-flow and associated ash-cloud surge deposits from the 8 and 20 May 1902 eruptions of Mt Pelée, and their inferred flow directions. The main block and ash-flow lobe fills the Rivière Blanche. Note how at Fond Canonville ash cloud surges moved around the ridge and then in an opposite direction to the main flow. (After Fisher *et al.* 1980, Fisher & Heiken 1982.)

(1981a) and C. J. N. Wilson and Walker (1982) suggested that some crystal- and lithic-rich deposits at the bottoms of some ignimbrite flow units are generated *within* the flow-head. These occupy the same stratigraphic position as the ground surge, but they are not deposited from a separate, dilute low-concentration flow, therefore not by a pyroclastic surge. G. P. L. Walker *et al.* (1981a) suggested that these deposits be called ground layers. They described one from the Taupo ignimbrite (Ch. 7), and suggested that some other examples of deposits previously called ground surges were deposited by this alternative mechanism. Towards the vent, the quite remarkable ground layer of the Taupo ignimbrite passes into a coarse-grained breccia (it contains blocks >1 m in diameter near the vent), and nearly always lacks internal stratification. On the other hand, ground surges are never as coarse-grained, and have well developed planar stratification or low angle cross-stratification. However, criteria to distinguish the deposits generated by all of these different mechanisms have not been clearly identified.

Ash-cloud surges are turbulent, low density flows generated in the overriding gas and ash cloud as observed above historic pyroclastic flows (Fig. 5.10). The towering ash cloud contains material elutriated from the top of the moving pyroclastic flow, which forms a basal underflow (Figs 5.11 & 13). However, most of the ash rising into the ash cloud is deposited later as a fine-grained ash-fall deposit. In some cases ash-cloud surges could become detached from the moving pyroclastic flow and move independently.

Fisher (1979) discussed the formation of ash-cloud surges in the Upper Bandelier ignimbrite. Fisher *et al.* (1980) and Fisher and Heiken (1982) discussed their formation during the Mt Pelée 1902 eruption. They suggest that block and ash flows were confined to valleys, while fully turbulent, dilute high energy ash-cloud surges moved down the mountain continually expanding outwards (Fig. 5.20). Gravity segregation within individual ash-cloud surges occurred as they expanded, resulting in secondary block and ash underflows with high particle concentrations, which did not travel as far. Fragment-depleted ash-cloud surges are thought to have devastated St Pierre. Burnt wood and other high temperature effects in St Pierre indicate that the flows were hot. The deposits only had a maximum thickness of 1 m in St Pierre, where they are fine-grained, and generally massive, but internal stratification can be found. However, G. P. L. Walker (1983) has questioned the *ash-cloud* interpretation of these deposits, and in some ways has reverted back to older ideas by suggesting

they were high-concentration blasts similar to that at Mt St Helens (Ch. 7). Ash-cloud surges and their deposits were certainly observed to develop at Mt St Helens 1980, and are described by Rowley *et al.* (1981).

5.6.3 SURGES ASSOCIATED WITH FALLS

There is evidence that some pyroclastic surges, associated with magmatically erupted air-fall deposits, are formed by the collapse of an eruption column (or margins of it) without the generation of an accompanying pyroclastic flow. Such surges would again be termed ground surges (Fisher 1979). Roobol and Smith (1976) described prehistoric 'pumice and crystal ground surge deposits' inter-bedded with pumice fall deposits on Mt Pelée, extending up to 2 km away from the vent, and suggested that they formed by gravity collapse of plinian eruption columns. No doubt surges found interbedded with pumice-fall deposits can be generated by other mechanisms. For example, small amounts of external water gaining access to the erupting magma (from surface ground water or a deep aquifer) could generate hot, dry base surges (Sheridan & Wohletz 1981). Sheridan *et al.* (1981) suggested surge deposits interbedded with the early erupted pumice-fall deposit of the AD 79 Vesuvius eruption (the Pompeii pumice of Lirer *et al.* (1973); Ch. 6) were formed in this way; these surges were generated before the major phreatomagmatic activity which produced the wet base surges and phreatoplinian layers mentioned previously.

5.7 Pyroclastic surge deposits: types and descriptions

From the above description, pyroclastic surge deposits can be divided into three types:

base-surge deposits
ground-surge deposits
ash-cloud surge deposits

5.7.1 BASE-SURGE DEPOSITS

Base surges produce stratified, laminated, sometimes massive deposits containing juvenile fragments, ranging from vesiculated to non-vesiculated cognate lithic clasts, ash, crystals and occasional accessory lithics. Large ballistic lithics may form bomb sags close to the vent. Surges produced in phreatic eruptions are composed almost totally of accessory lithics, plus perhaps minor amounts of accidental lithics. Juvenile fragments are usually less than 10 cm in diameter, due to the high degree of fragmentation caused by the water–magma interaction. Base surges can accumulate thick deposits (>100 m) around some phreatomagmatic craters (Ch. 13), although they thin rapidly away from the vent. Deposits found in the successions of stratovolcanoes are generally thin (<5 cm to <5 m). Internally, deposits show unidirectional bedforms, and climbing dune-forms can be common (Figs 5.21a, b & 22). Near vent it may be difficult to distinguish planar-bedded surge deposits from

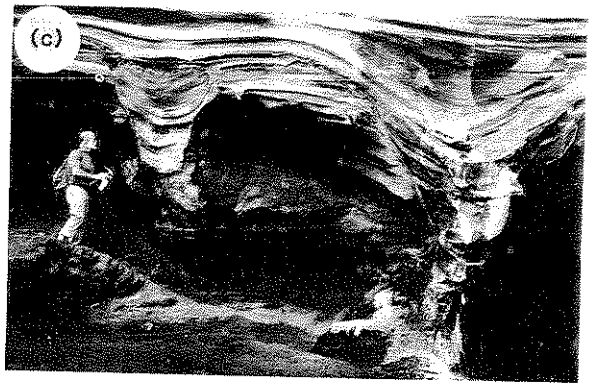

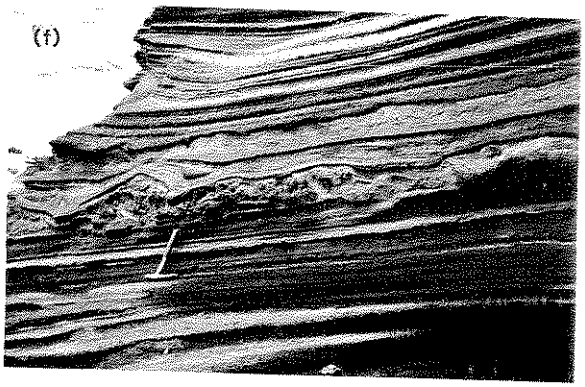

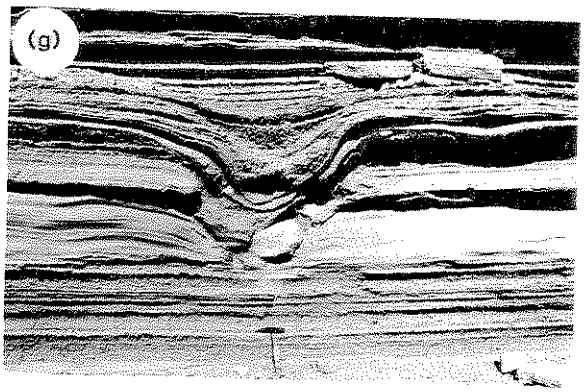

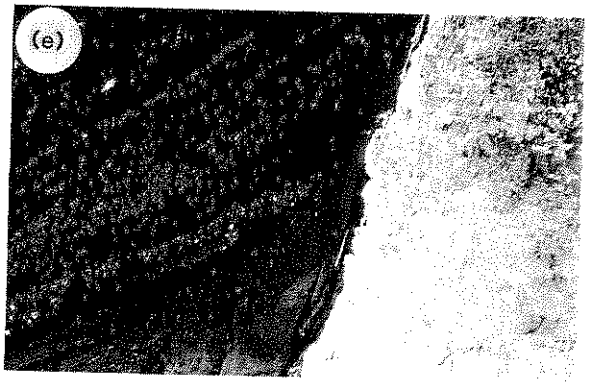

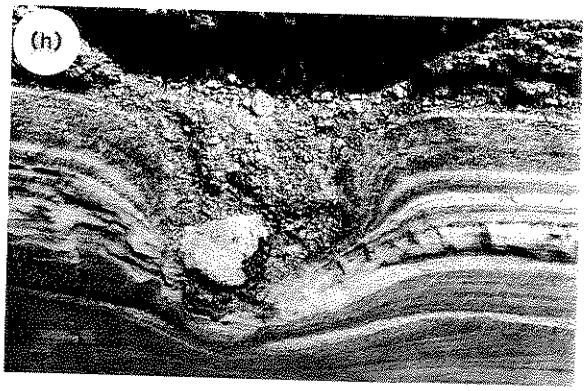

Figure 5.21 Some features of basaltic base-surge deposits. (a) Climbing duneforms, surge flow direction from right to left. Thin planar layers are air-fall deposits. From Lake Purrumbete maar, Western Victoria, Australia. (b)–(f) are from the coastal slopes of Koko crater, Oahu, Hawaii, but most of the deposits in this area are thought to have been erupted from the Hanauma Bay crater complex, 1–5 km to the southwest. (b) Climbing duneforms, surge direction left to right from Hanauma Bay, Hawaii. (c) and (d) U-shaped erosional channels; U-shaped bases and stratigraphy of the deposits suggest that these were fluviatile erosional gullies reshaped and re-emphasised by younger base surges from Hanauma Bay. (For complete story see Fisher 1977.) Note how planar-bedded base surge layers thicken into the channels (cf. Fig. 5.1c). (e) Ash plastered against the almost vertical side of a wall of eroded basement of reef limestone. (f) Planar bedded deposits with penecontemporaneous slumping. (g) and (h) Bomb sags in planar-bedded deposits, Tower Hill, Victoria.

ated, some-
venile frag-
-vesiculated
l occasional
s may form
oduced in
st totally of
amounts of
are usually
high degree
ter–magma
ilate thick
omagmatic
pidly away
cessions of
< 5 cm to
directional
e common
be difficult
osits from

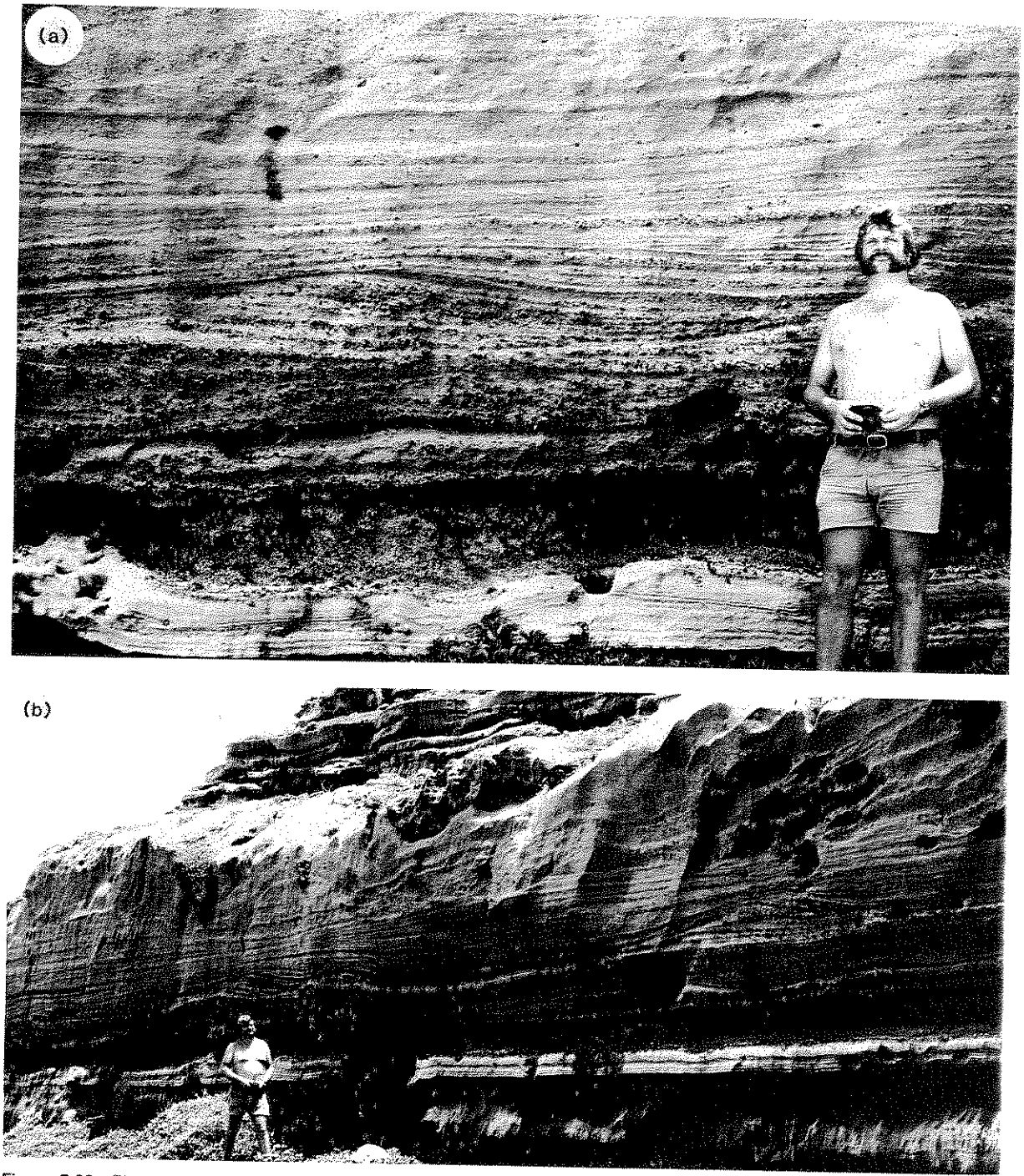

Figure 5.22 Rhyolitic base-surge deposits erupted from the Quill, St Eustatius (<22 240 years BP), Lesser Antilles. The base-surge deposits dominate the stratigraphic interval visible in (a). Here there is a thin lower unit of base-surge deposits (prominent white layer) separated from the thicker upper unit with well developed dunes by a plinian pumice-fall deposit. The more-massive layer above these shown in (b) is a co-eruptive ignimbrite.

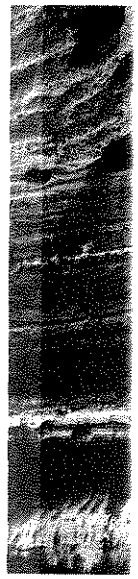

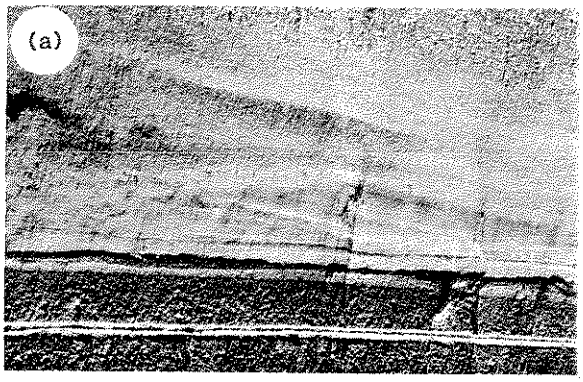

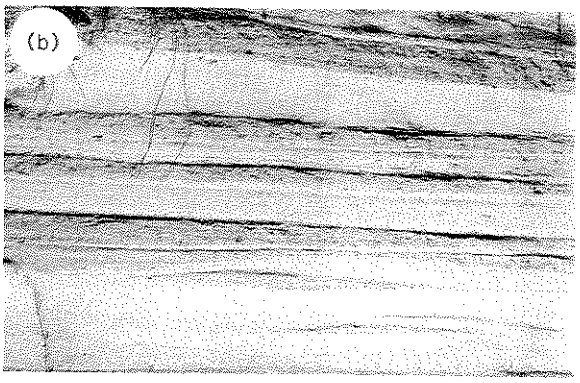

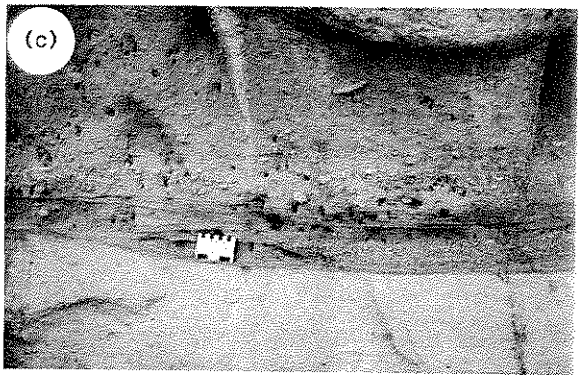

Figure 5.23 Some ground surge and ash-cloud surge deposits. (a) and (b) Ground surge deposits at the base of the Upper Bandelier ignimbrite. (c) Ground surge deposit separating two flow units in the Upper Bandelier ignimbrite. The dark (pink) stratified surge deposit is clearly associated with the upper darker flow unit and they were emplaced as one thermal package. (d) Ash-cloud surge deposits between two flow units of the Upper Bandelier ignimbrite. Local field relations and the photograph show that the thinly laminated surge deposits are associated with the pumice-rich top of the lower flow unit (cavernous weathering). (e) Fine-grained 1902 ash-cloud surge deposit in the churchyard at St Pierre. Internal stratification is found in this. (f) The church at St Pierre is thought to have been destroyed by an ash-cloud surge.

...s. The base-
...rge deposits
...deposit. The

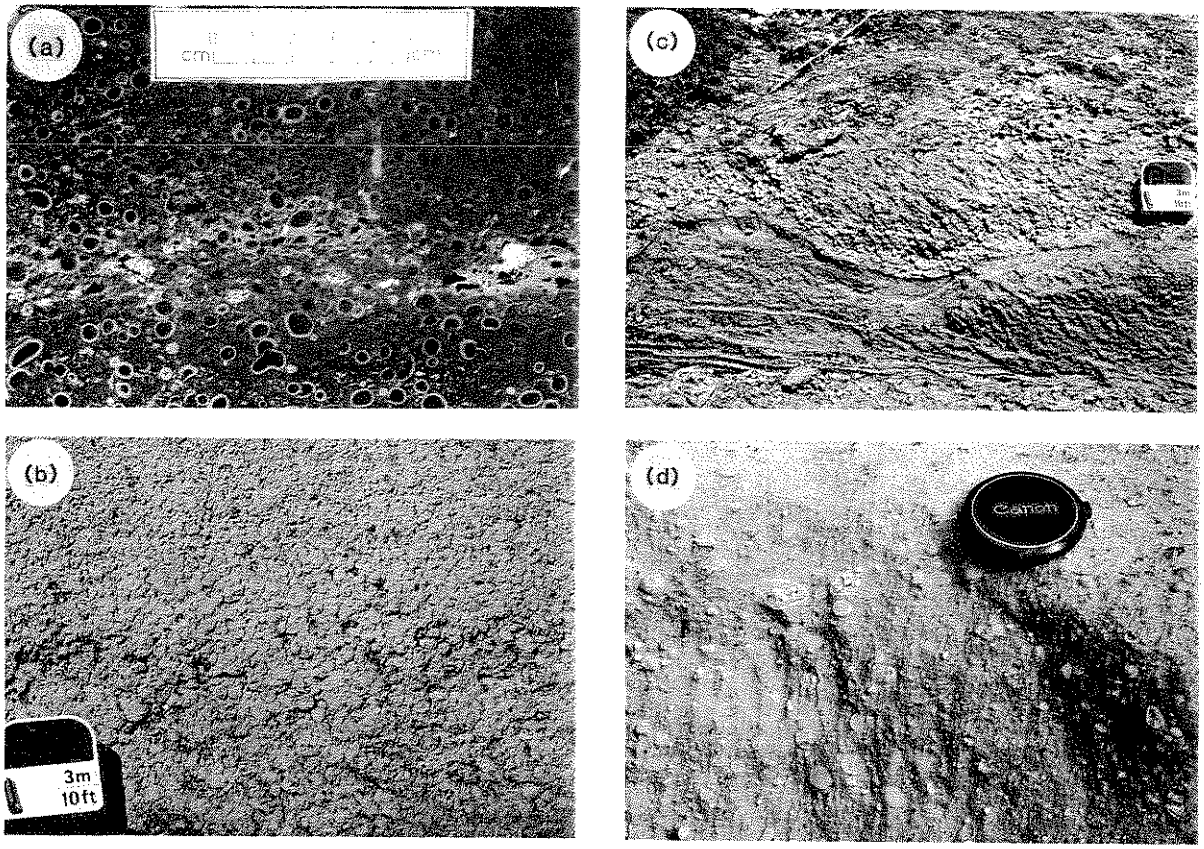

Figure 5.24 (above and facing page) Accretionary and cored lapilli. (a)–(f) Associated with different rhyolitic deposits. (a) Within a rhyolitic ignimbrite from the Devonian Snowy River Volcanics, eastern Victoria, Australia. The matrix contains an abundance of flattened and fragmented lapilli. (b) and (c) show exceptional concentrations of accretionary lapilli from phreatoplinian air-fall ashes of the Oruanui eruption, Lake Taupo, deposited in a small crater lake inside the scoria cone, Pukeonake, New Zealand. These have been reworked, as shown by the erosion surface in (c). (d) Lapilli within an ignimbrite about 500 000 years BP in New Zealand (photograph by C. J. N. Wilson). (e) In gas segregation pipes within the Oruanui ignimbrite, New Zealand. (f) From a thick concentration of accretionary lapilli within the body of the Oruanui ignimbrite. (g) Cored lapilli at Koko Crater, Oahu, Hawaii. (h) Cored lapilli in basaltic base surge deposits at Cape Bridgewater volcano, Victoria.

flat-bedded air-fall deposits. Surge deposits usually show some low-angle truncations, and therefore these are key features to look for (criteria to distinguish these two types of deposit in such situations are discussed further in Ch. 7). U-shaped erosional channels have also been described (Figs 5.21c & d) and their formation has been discussed by Fisher (1977).

Base-surge deposits often show evidence of being wet and 'sticky' when deposited. Accretionary lapilli are common (Section 5.8). Deposits may be plastered and stuck to vertical or almost vertical surfaces (Fig. 5.21e), and layers often deform plastically, which can be seen when large bombs impact (Figs 5.21g & h), or there is penecontemporaneous slumping (Fig. 5.21f). Also, vesiculated tuffs with entombed gas cavities may be present. Note, however, that vesiculated tuffs are not solely diagnostic of a base-surge origin as indicated by Lorenz (1974), and can be found in phreatomagmatic ash-fall layers, and not necessarily near the vent. They only show that ash was nearly saturated

deposits. (a)
contains an
lapilli from
scoria cone,
an ignimbrite
the Oruanui
ignimbrite. (g)
later volcano.

ost vertical
en deform
rge bombs
necontem-
vesiculated
be present.
e not solely
dicated by
hreatomag-
ly near the
ly saturated

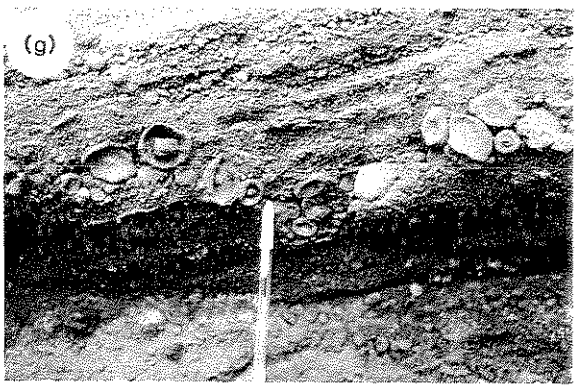

with water at the time of deposition, and that trapped air or steam could not escape. When basaltic in composition, juvenile material is usually, to some extent, hydrated and altered to palagonite (Chs 13 & 14). Such deposits can be lithified, but should not be confused with welded tuffs.

5.7.2 GROUND-SURGE DEPOSITS

Ground surges produce stratified deposits generally less than 1 m thick which are typically recognised at the base of pyroclastic flow units (Figs 5.23a, b & c). The deposits are composed of ash, juvenile

vesiculated fragments, crystals and lithics in varying proportions, depending on the constituents present in the eruption column. They are typically enriched in denser components (less well vesiculated juvenile fragments, crystals and lithics) compared with accompanying pyroclastic flow deposits (Sparks 1976). Again, they show unidirectional bedforms; carbonised wood and small gas segregation pipes may be present.

5.7.3 ASH-CLOUD SURGE DEPOSITS

The products of ash-cloud surges are stratified deposits generally less than 1 m thick found at the top of, and as lateral equivalents to pyroclastic flow units (Figs 5.23d & e). They show unidirectional bedforms and pinch and swell structures, and may occur as discrete separated lenses (Fisher 1979). The grainsize and proportions of components depend on the type of the parent pyroclastic flow. One would intuitively expect such deposits to be enriched in vitric particles. However, those associated with the Bandelier Tuffs (Fisher 1979; Fig. 5.23d) are enriched in crystals, and this must be due to further gravity segregation within the ash cloud, as ash-sized particles with a significant proportion of crystals are elutriated out of the parent pumice flow. The ash cloud surges described by Fisher and Heiken (1982) from the 1902 eruption of Mt Pelée (Fig. 5.23e) have very similar component proportions to both their parent and secondary block and ash flows, but this is not surprising because there is little density difference between dense ash-sized juvenile fragments and crystals. Ash-cloud surge deposits again can contain small gas segregation pipes.

5.8 Accretionary lapilli

Accretionary lapilli are lapilli-sized pellets of ash commonly exhibiting a concentric internal structure (J. G. Moore & Peck 1962; Fig. 5.24a). They have been described from pyroclastic fall, surge and flow deposits. They are believed to form by the accretion of fine ash around some nucleus, either a water droplet or solid particle. This could occur during rain flushing (J. G. Moore & Peck 1962, G. P. L. Walker 1981a) either of the downward plume from an eruption column or of the accompanying ash cloud of a pyroclastic flow. However, perhaps more frequently, they form in the steam-rich columns of phreatomagmatic and phreatic eruptions (Self & Sparks 1978; the examples shown in Fig. 5.24a), perhaps around consensing water droplets. They can then be transported and deposited by fall, base surge or flow processes. Basaltic base-surge deposits often seem to contain the variety called **cored** or **armoured lapilli**, which have a recognisable lithic core and a thick (sometimes 1–2 cm) shell of unstructured ash (Figs 5.24g & h). Perhaps these form in the outward-moving base-surge cloud as solid fragments pick up a coating of sticky wet ash. Accretionary lapilli also form by gases streaming up through pyroclastic flow deposits, and they occur in segregation pipes (G. P. L. Walker 1971; Figs 5.24e & f).

It is important to stress that accretionary lapilli *are not indicative* solely of pyroclastic fall deposits, as often seems to be assumed by workers in ancient successions. They may occur in pyroclastic fall, flow or surge deposits. Indeed, stratified deposits several metres thick, with accretionary lapilli, are more likely to be base-surge deposits. Also, some accretionary lapilli can survive a limited amount of reworking and redeposition, and can therefore be found in epiclastic volcanic sediments (Figs 5.24b & c). Furthermore, they can form *well away from vents* in pyroclastic flows and their trailing ash clouds, as well as in secondary eruption columns generated when pyroclastic flows interact explosively with surface water into which they flow (Chs 8 & 9). They are therefore not indicative of exclusively near-vent depositional settings.

5.9 Further reading

Aspects of the geology of pyroclastic deposits are fully developed and discussed in our later chapters. In Chapter 12 we will present a classification, and in Chapter 12 and Appendix II we consider criteria that may distinguish these rocks in ancient volcanic successions.